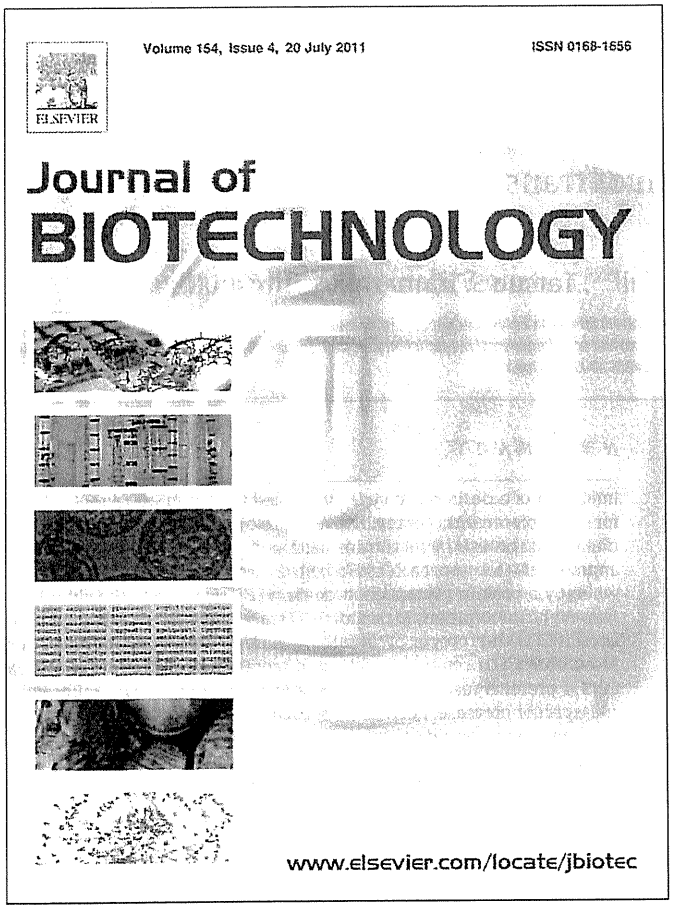

Journal of Biotechnology 154 (2011) 298–303

Contents lists available at ScienceDirect

Journal of Biotechnology

journal homepage: www.elsevier.com/locate/jbiotec

Short communication

Intracellular reactivation of transcription factors fused with protein transduction domain

Masamitsu Konno[a], Shinji Masui[b,c], Tatsuo S. Hamazaki[a], Hitoshi Okochi[a,*]

[a] Department of Regenerative Medicine, Research Institute, National Center for Global Health and Medicine, 1-21-1 Toyama, Shinjuku-ku, Tokyo 162-8655, Japan
[b] Section of Molecular Biology and Cell Engineering, Department of Regenerative Medicine, Research Institute, National Center for Global Health and Medicine, Tokyo 162-8655, Japan
[c] PRESTO, Japan Science and Technology Agency, Saitama 332-0012, Japan

ARTICLE INFO

Article history:
Received 10 May 2011
Accepted 13 May 2011
Available online 23 May 2011

Keywords:
PTD
iPS cells
ES cells
Oct3/4
Sox2
TEV protease

ABSTRACT

Induction of a desired cell type by defined transcription factors (TFs) using iPS technology can be used for cell replacement therapy. However, to overcome problems such as tumor formation, genomic insertional mutagenesis by viral transduction in the induction process needs to be avoided using alternative approaches. One approach could be the direct delivery of TF protein by a protein transduction system, whereby a protein transduction domain (PTD) is fused to facilitate the penetration of cell membrane. However, fusion proteins, including TFs, are reported to be biologically less active through the interference of PTD with proper protein folding. Here, we report a proof-of-concept study in which TF proteins fused with PTDs could be reactivated by removal of PTDs from cells. We demonstrated that Sox2 and Oct3/4 proteins fused with PTD were less active in mouse embryonic stem cells. Removal of PTD by a site-specific protease, derived from tobacco etch virus (TEV), substantially restored the functionality of these proteins, proved by enhanced rescue ability for differentiation induced by endogenous *Sox2* and *Oct3/4* repression. These results suggest that, by removing a PTD inside the cells, directly delivered TF proteins may exert substantially enhanced function than presently considered.

1. Introduction

Transcription factors (TFs) regulate gene expression, and some play pivotal roles in the determination of a cellular differentiation status. In a pioneer study, Davis et al. (1987) showed that the basic helix–loop–helix (bHLH) transcription factor MyoD induced muscle-specific properties in fibroblasts. Recent examples include induction of pancreatic β-cells from adult pancreatic exocrine cells by Ngn3, Pdx1, and Mafa (Zhou et al., 2008), neural cells from fibroblasts by Ascl1, Brn2, and Myt1l (Vierbuchen et al., 2010), macrophages from fibroblasts by PU.1 and Cebpa (Feng et al., 2008), and myocardial cells from fibroblasts by Gata4, Mef2c, and Tbx5 (Ieda et al., 2010). In addition to lineage switching between differentiated cell types, introduction of TFs can induce dedifferentiation by four TFs including Oct3/4 and Sox2 (Takahashi and Yamanaka, 2006). Retrovirus or lentivirus is employed for introduction of these TFs; however integration into the host genome can lead to insertional mutagenesis and unpredictable gene activation (Okita et al., 2007). Thus, at present, these methods are unsuitable for clinical trials or pathological analysis (Hanna et al., 2007; Wernig et al., 2008).

As an alternative to viral transduction, a protein transduction system for direct delivery of TFs into target cells has been developed. To facilitate the penetration of cell membrane, fusion with a high proportion of basic amino acids, termed a protein transduction domain (PTD), is required. PTDs, reported to date include TAT derived from HIV virus (Frankel and Pabo, 1988), Antenapedia transcription factor from *Drosophila* (Derossi et al., 1996), VP22 structural protein of Herpes-simplex virus 1 (Phelan et al., 1998), and poly-arginine (Matsushita et al., 2001; Wender et al., 2000). Although protein-fused PTD such as 11R (arginine)-P53 or VP22-P53 could penetrate cells (Phelan et al., 1998; Takenobu et al., 2002), it was also pointed out that these fusion proteins were biologically less active because of the improper folding of the protein caused by PTD (Ye et al., 2002). The efficiency of establishing iPS cells by Oct3/4, Sox2, Klf4, and c-Myc protein-fused 8R (arginine) was quite low (Kim et al., 2009). Therefore, we hypothesized that PTD should be removed from cells, especially PTD fused with TF.

In this study, we employed a site-specific protease, derived from tobacco etch virus (TEV), to dissociate PTD from fusion protein in the cell. Because of the stringent sequence specificity, TEV protease has been employed in cleaving genetically engineered fusion proteins in vitro (Dougherty et al., 1988). We demonstrated that TEV

* Corresponding author. Tel.: +81 3 3202 7181x2825; fax: +81 3 3202 7192.
E-mail address: hokochi@ri.ncgm.go.jp (H. Okochi).

0168-1656/$ – see front matter © 2011 Elsevier B.V. All rights reserved.
doi:10.1016/j.jbiotec.2011.05.006

protease introduced into mouse embryonic stem (ES) cells were effective in restoring the function of TF proteins by removal of PTD, suggesting that directly delivered TF proteins may generally exert substantially enhanced functionality than presently considered.

2. Materials and methods

2.1. Cell culture

Mouse ES cells, 2TS22C, ZHBTc4, and Plat-E cells, were cultured according to the methods described by Masui et al. (2007), Niwa et al. (2000), and Morita et al. (2000), respectively.

2.2. Plasmid construction

An eleven arginine (11R) codon sequence was combined with cDNA of *Sox2* or *Oct3/4* to obtain 11RSox2 or 11ROct3/4 (Fig. 1A). Each construct was cloned into pPy vector with CAG-IB or CAG-IP to obtain pPyCAG-IB/11RSox2 or pPyCAG-IP/11ROct3/4. The TEV protease recognition sequence was inserted between the 11R sequence and *Sox2* or *Oct3/4* to obtain pPyCAG-IB/11RTEVRSox2 or pPyCAG-IP/11RTEVROct3/4 (Fig. 1C). The residual sequence after cleavage by TEV protease was ligated with the *Sox2* or *Oct3/4* sequence to obtain pPyCAG-IB/ΔTEVRSox2 or pPyCAG-IP/ΔTEVROct3/4 (Fig. 1B). These plasmids were generated through the following steps. For pPyCAG-IB/11RSox2, the 11R-Sox2 cDNA was amplified from pBRCAGIH/Sox2 using PCR with the primers 5′-11RSox2 (5′-ATACTCGAGCCACCATGGACGCAGGCGAAGGCGACGGGAGAATCTG-TACTATGGGTGATATCCAATGTATAACATGAT-3′ [XhoI site is underlined]) and 3′-Sox2 (5′-ACAGCGGCCGCTCACATGTGCGACAGGGG-CA-3′ [NotI site is underlined]). For pPyCAG-IB/ΔTEVRSox2, the ΔTEVRSox2 cDNA was amplified from pBRCAGIH/Sox2 using PCR with the primers 5′cutSox2 (5′-ATACTCGAGCCACCATGGGTGA-TATCCAATGTATAACATGAT-3′ [XhoI site is underlined]) and 3′-Sox2. For pPyCAG-IB/11RTEVRSox2, the 11RTEVRSox2 cDNA was amplified from pBRCAGIH/Sox2 using PCR with the primers 5′-11RTEVRSox2 (5′-ATACTCGAGCCACCATGGACGCAGGCGAAGG-CGACGGGAGAATCTGTACTTCCAGGGTGAGAATCTGTACTTCCAGG-GTGAGAATCTGTACTTCCAGGGTGAGAATCTGTACTATGGGTGATAT-CCAATGTATAACATGAT-3′ [XhoI site is underlined]) and 3′-Sox2. For pPyCAG-IP/11ROct3/4, the 11ROct3/4 cDNA was amplified from pBRCAGIH/Oct3/4 using PCR with the primers 5′-11ROct3/4 (5′-ATACTCGAGCCACCATGGACGCAGGCGAAGGCGACGGGAGAATCTG-TACTATGCCCACGTTCGACCAGGC-3′ [XhoI site is underlined]) and 3′-Oct3/4 (5′-ACAGCGGCCGCTCAGACATCAGAAGTAGAAA-3′ [NotI site is underlined]). For pPyCAG-IP/11RTEVROct3/4, the 11RTEVROct3/4 cDNA was amplified from pBRCAGIH/Oct3/4 using PCR with the primers 5′-11RTEVROct3/4 (5′-ATACTCGAGCC-ACCATGGACGCAGGCGAAGGCGACGGGAGAATCTGTACTTCCAGGG-TGAGAATCTGTACTTCCAGGGTGAGAATCTGTACTTCCAGGGTGAGA-ATCTGTACTATGCCCACGTTCGACCAGGC-3′ [XhoI site is underlined]) and 3′-Oct3/4. For pPyCAG-IP/ΔTEVROct3/4, the ΔTEVROct3/4 cDNA was amplified from pBRCAGIH/Oct3/4 using PCR with the primers 5′-ΔTEVROct3/4 (5′-ATACTCGAG-CCACCATGCCCACGTTCGACCAGGC-3′ [XhoI site is underlined]) and 3′-Oct3/4. These cloning products were digested with XhoI and NotI.

Three different mutations in TEV protease cDNA were combined with drug resistance genes for hygromycin or histidinol. Six plasmid constructs, pMYsIH/TEV protease S219D mutant, pMYsIH/TEV protease S219P mutant, pMYsIH/TEV protease S219V mutant, pMYsIHisD/TEV protease S219D, pMYsIHisD/TEV protease S219P, and pMYsIHisD/TEV protease S219V mutant were generated through the following steps. For pMYsIH/TEV protease S219D and pMYsIHisD/TEV protease S219D, the TEV protease S219D cDNA was amplified from pRK603 (Addgene) using PCR with the primers 5′-S219D (5′-TTTGTCGACATGGGAGAAAGCTTGTTTAA-3′ [SalI site is underlined]) and 3′-S219D (5′-TTTGCGGCCGCATTAATTCATGAGTTGAGTC-3′ [NotI site is underlined]). For pMYsIH-IH/TEV protease S219P or S219V and pMYsIHisD/TEV protease S219P or S219V, the TEV protease S219P or S219V cDNA was amplified from pRK792 (Addgene) or pRK793 (Addgene) using PCR with the primers 5′-S219P (5′-TTTGTCGACGGTCATCATCATCATCATCA-3′ [SalI site is underlined]) and 3′-S219D (5′-TTTGCGGCCGCTTAGCGACGGCGACGACGAT-3′ [NotI site is underlined]).

2.3. Retroviral infection

Retroviral supernatant were prepared from Plat-E cells as described by Takahashi and Yamanaka (2006). Two days after infection, we initiated selection of 2TS22C using 0.1 mg/ml hygromycin (Invivogen) or ZHBTc4 using 3 mM histidinol (Sigma). The selection of clones was performed over a period of 2 weeks.

2.4. RT-PCR

The expression of TEV protease gene and the pluripotency marker genes *Oct3/4* and *Nanog* was determined by RT-PCR. Total RNA was extracted using Isogen (Nippon Gene) as described by the manufacturer and then treated with High-Capacity RNA-to-cDNA kit (AB gene) to generate cDNA. Then PCR amplification was performed for the three types of TEV protease mutant gene. PCR cycles were as follows: 95 °C for 5 min, 95 °C for 30 s, annealing temperature for 30 s, 72 °C for 1 min (25–30 cycles), and 72 °C for 3 min. The RT-PCR products were analyzed using 1% agarose gel electrophoresis and visualized with ethidium bromide. Primers used in this study are *TEVprotease* (S219V and S219P) (5′-CACTCAGCATCGAATTTCACCAA-3′ and 5′-GCTGAAAAGGCTCTTCAGGTTTC-3′), *TEVprotease* (S219D) (5′-TACA-CTCAGCATCGAATTTCACCAA-3′ and 5′-AAAAGGCTCTTCAGGTTT-GTCCA-3′), *GAPDH* (5′-TGAAGGTCGGTGTGAACGGATTTGGC-3′ and 5′-CATGTAGGCCATGAGGTCCACCA-3′), and *Nanog* (5′-GTAGC-TGTCTTCAGACACTCC-3′ and 5′-AATTAGAGCTATGCAGAGAAA-3′).

2.5. TF rescue experiment

Sox2 and *Oct3/4* repression was induced by the addition of tetracycline (Tc) (1 μg/ml) to 2TS22C and ZHBTc4 culture media (Masui et al., 2007; Niwa et al., 2000). Plasmids containing various forms of TFs (Fig. 1) were introduced to these cells using lipofectamin 2000 (Invitrogen) according to the manufacturer's recommendations. Cells were replated in Tc^+ or Tc^- media and selected for 2TS22C cells using 10 μg/ml blasticidin S (Invivogen) for 14 days or for ZHBTc4 cells using 1 μg/ml puromycin (Invivogen) for 10 days. Colonies identified by Leishman (Sigma, St Louis, MO) staining were counted. The rescue index of a given cDNA was determined by the ratio of colonies in Tc^+ to those in Tc^- media after subtracting the ratio of empty vector (background), which was then normalized by the ratio of *Sox2* or *Oct3/4* expression vector (positive control).

3. Results

3.1. PTDs interfere with the function of Sox2 and Oct3/4

To investigate whether Sox2 fused with PTD retained its normal function, we employed a functional complementation system based on the drug-inducible Sox2 knockout ES cells, 2TS22C. Here, endogenous *Sox2* is repressed in 2TS22C upon addition of Tc, which leads to differentiation of these cells and to reduction in colony-forming capacity (reflected in colony number). The number of

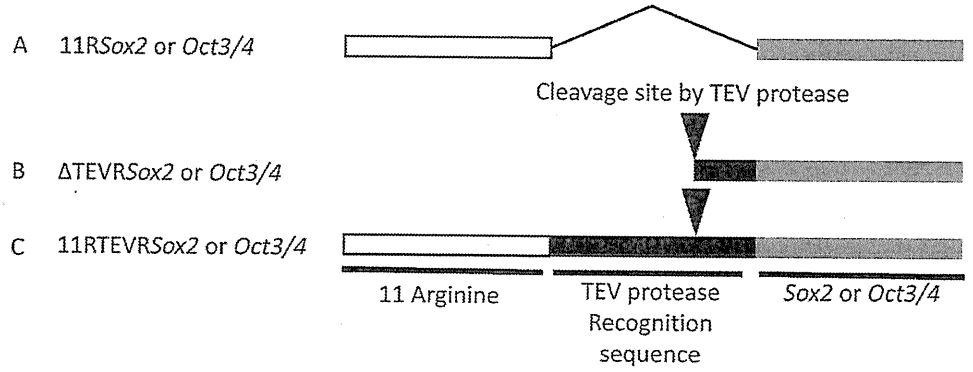

Fig. 1. Expression vectors used in the rescue experiments. (A) An eleven arginine (11R) sequence codon was ligated with *Sox2* or *Oct3/4* cDNA, (B) the residual sequence after cleavage of TEV protease was ligated with *Sox2* or *Oct3/4* cDNA, and (C) a TEV protease recognition sequence was inserted between the 11R sequence and *Sox2* or *Oct3/4* cDNA.

colonies increases only when exogenously introduced *Sox2* is functional (Masui et al., 2007). The normalized ratio of colony number, termed rescue index, reflects the relative activity of exogenous *Sox2*. When 11R or VP22 as a PTD was fused with Sox2, the rescue indices were greatly reduced compared with wild-type Sox2, suggesting that PTD interfered with the function of Sox2 (Table 1). Conversely, Sox2 fused with the residual sequence of the TEV protease recognition site showed an enhanced rescue index, suggesting that cleavage between PTD and Sox2 by TEV protease will be able to restore the function.

Next, to examine whether PTD disturbs the function of another TF, we assayed Oct3/4 fused with PTD in ZHBTc4, which represses endogenous *Oct3/4* expression in Tc^+ and loses colony-forming capacity. As in the case of Sox2, Oct3/4 fusion with 11R greatly reduced its function, whereas in the case of Oct3/4 without 11R (with the residual sequence of the TEV protease recognition site), the function was restored substantially (Table 1). These results suggest that the addition of PTD to TFs compromises the function of TFs, whereas intracellular removal of PTD by TEV protease restores the function.

3.2. Expression of TEV protease in ES cells does not compromise pluripotent stem cell specific gene expression

Wild-type TEV protease is known to be unstable because of its self-cleaving activity. More stable and efficient TEV protease mutants have been developed (Kapust et al., 2001), which are reported to be active in a variety of species including *E. coli* (Kapust and Waugh, 2000), yeast (Rigaut et al., 1999), *Drosophila* (Pauli et al., 2008), *Xenopus* (Wawersik et al., 2005) and rat (Wehr et al., 2006). To establish mouse ES cells expressing TEV protease, we infected mouse ES cells (2TS22C or ZHBTc4) with retroviruses carrying three types of TEV protease mutant (TEV-S219D, TEV-S219P or TEV-S219V). We confirmed that these ES cells expressed transgenes for TEV protease mutants (Fig. 2A). We then checked for the expression level of *Nanog*, marker gene for pluripotency, and found that they were maintained at almost the same level as the wild-type (Fig. 2B), suggesting that TEV protease did not cleave endogenous proteins necessary to maintain cellular identity.

Table 1
PTDs interfere with TF function.

Vectors	Tc^+ (Sox2 null)	Tc^-	Rescue index
(A) 2TS22C			
pPyCAGIB	22	344	0
pPyCAGSox2IB	270	286	1.0
pPyCAGIB/VP22Sox2	49	466	0.07
pPyCAGIB/11RSox2	57	436	0.09
pPyCAGIB/Δ TEVR-Sox2	162	258	0.63
Vectors	**Tc^+ (Oct3/4 null)**	**Tc^-**	**Rescue index**
(B) ZHBTc4			
pPyCAGIP	3	603	0
pPyCAGOct3/4IP	256	285	1.0
pPyCAGIP/11ROct3/4	8	216	0.03
pPyCAGIP/Δ TEVR-Oct3/4	248	298	0.93

The results of assay in 2TS22C (A) and ZHBTc4 (B). Colony numbers are shown in Tc^+ and Tc^- column.

3.3. TEV protease-expressing ES cells can restore the function of Sox2 fused with PTD

To address whether TEV protease can function in ES cells and contribute to restoring the function of TF by removing PTD, we introduced 11RSox2, ΔTEVRSox2, or 11RTEVRSox2 (containing TEV protease recognition site between 11R and Sox2) into wild-type 2TS22C or 2TS22C expressing the TEV protease mutants (2TS22C-TEVS219D, 2TS22C-TEVS219P or 2TS22C-TEVS219V). As

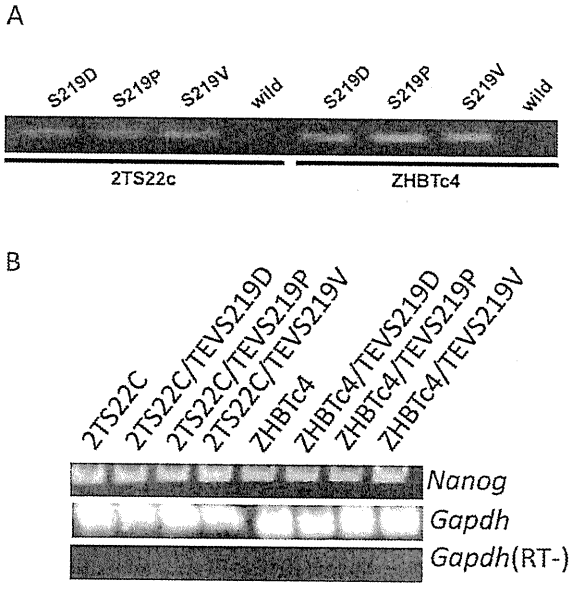

Fig. 2. Expression of TEV protease in ES cells does not compromise pluripotent stem cell specific gene expression. (A) RT-PCR analysis to confirm expression of transgenes for TEV protease mutants (S219D, S219P, S219V) and (B) RT-PCR analysis for *Nanog* in the ES cells.

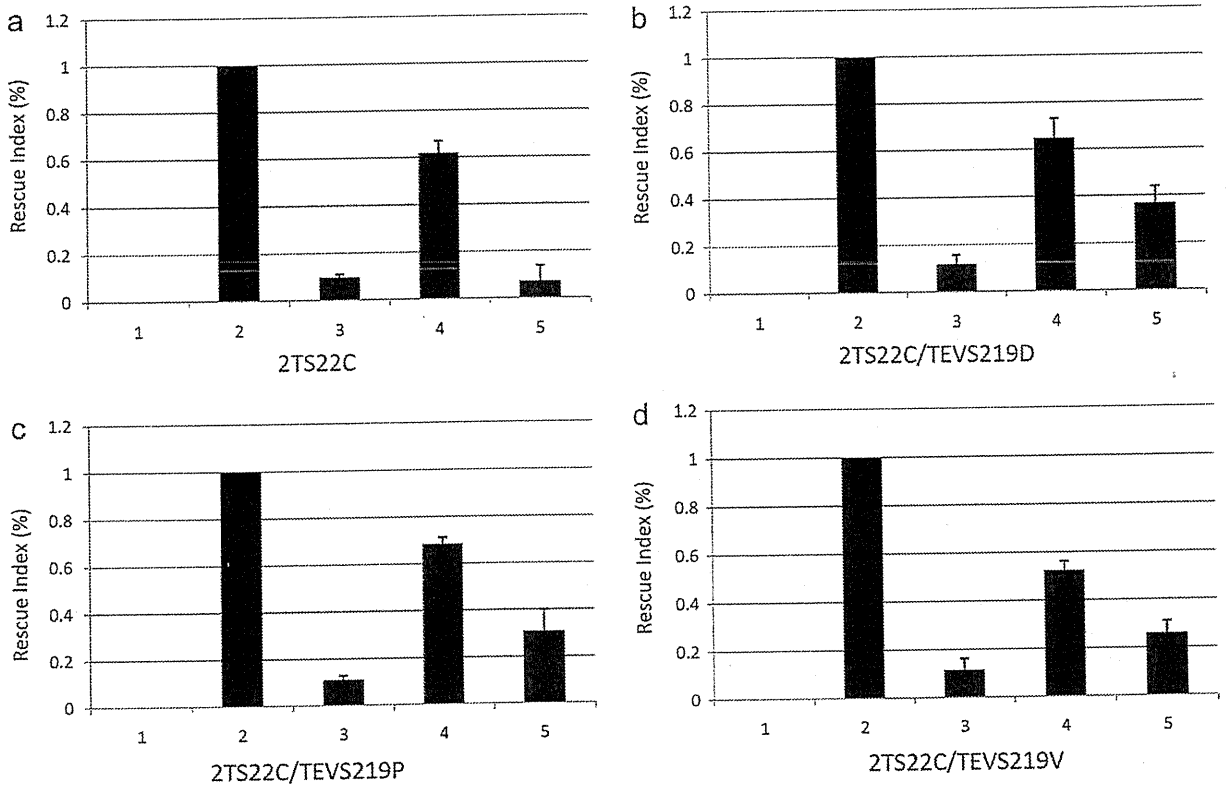

Fig. 3. TEV protease-expressing ES cells can restore the function of Sox2 fused with PTD. 1, pPyCAG-IB, empty vector; 2, pPyCAGSox2-IB; 3, pPyCAG-IB/11RSox2, 11R-containing Sox2; 4, pPyCAG-IB/ΔTEVRSox2, truncated form of Sox2 with residual fusion protein; 5, pPyCAG-IB/11RTEVRSox2, 11R-TEV recognition sequence-Sox2.

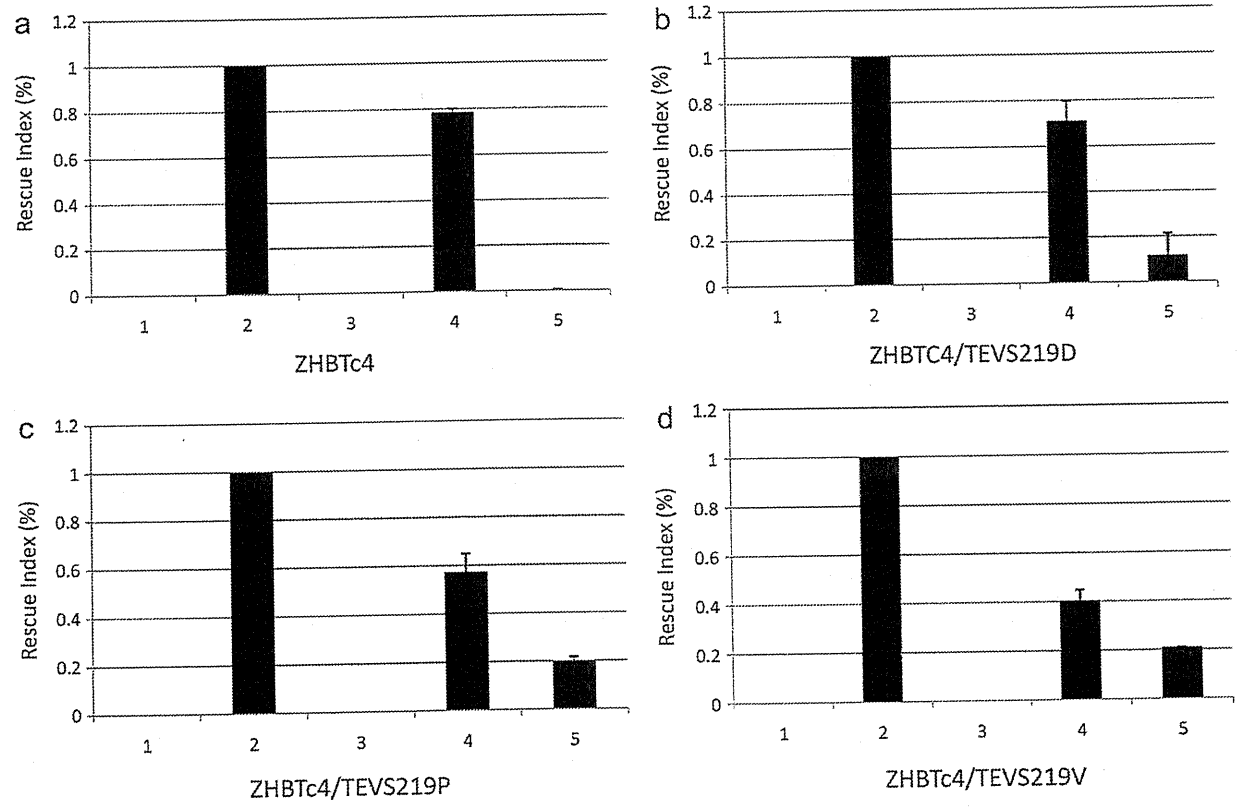

Fig. 4. TEV protease-expressing ES cells can restore the function of Oct3/4 fused with PTD. 1, pPyCAG-IP, empty vector; 2, pPyCAGOct3/4-IP; 3, pPyCAG-IP/11ROct3/4, 11R-containing Oct3/4; 4, pPyCAG-IP/ΔTEVROct3/4, truncated form of Oct3/4 with residual fusion protein; 5, pPyCAG-IP/11RTEVROct3/4, 11R-TEV recognition sequence-Oct3/4.

expected, the rescue index of 11RSox2 was greatly reduced (Fig. 3a–d, lane 3). In contrast, 11RTEVRSox2 substantially enhanced rescue index to a level comparable to that of ΔTEVRSox2 (Fig. 3b–d, lanes 4 and 5). This restoration of function was due to the activity of TEV protease, since no enhancement was observed in 2TS22C without the TEV protease transgene (Fig. 3a, lanes 4 and 5). These results indicate that the TEV protease cleaved 11RTEVRSox2 protein to remove PTD, which restored Sox2 function. The efficacy of the three TEV protease mutants was comparable.

3.4. TEV protease-expressing ES cells can restore the function of Oct3/4 fused with PTD

To determine whether the function of another TF can be recovered by removing the PTD, we introduced 11ROct3/4, ΔTEVROct3/4 or 11RTEVROct3/4 into wild-type ZHBTc4 or ZHBTc4 expressing the TEV protease mutants (ZHBTc4-TEVS219D, ZHBTc4-TEVS219P and ZHBTc4-TEVS219V). As expected, the rescue index of 11ROct3/4 was greatly reduced (Fig. 4a–d, lane 3). In contrast, 11RTEVROct3/4 substantially enhanced the rescue index to a level comparable to that of ΔTEVROct3/4 (Fig. 4b–d, lanes 4 and 5). This functional restoration was due to the activity of TEV protease, as no enhancement was observed in ZHBTc4 without the TEV protease transgene (Fig. 4a, lanes 4 and 5). These results indicate that TEV protease cleaved 11RTEVROct3/4 protein to remove PTD, which restored Oct3/4 function. The efficacy of the three TEV protease mutants was comparable.

Collectively, these results suggest that a PTD interferes with the function of TFs, which can be restored by intracellular removal of PTD by TEV protease.

4. Discussion

To date, there are three approaches to circumvent insertional mutagenesis in cellular induction experiments. (i) In a non-integration type DNA-based approach such as an episomal vector, occasional integration into the genome has been observed (Okita et al., 2008). Thus it is desirable to avoid introducing exogenous DNA into the cell. (ii) In an RNA-based approach, such as mRNA transfection (Warren et al., 2010), expression level may not be strong and continuous enough to induce global change in transcriptional profile. This may limit usefulness to general applications. In fact, a number of mRNA transfections are required for induction of iPS cells (Warren et al., 2010). Conversely, in Sendai virus (SeV), the RNA virus that does not integrate with the genome, transgene expression is known to be strong and continuous because SeV replicates in the cell (Li et al., 2000). Although it is known that SeV in the cells can be eliminated by using temperature-sensitive replication mutants of SeV (Inoue et al., 2003), for clinical use it will be difficult to achieve complete elimination from all the cells. This may result in unexpected effects of transgene TFs a long time after cell replacement therapy. (iii) A protein-based approach such as protein transduction, does not produce residual exogenous TFs upon withdrawal from the medium. In addition, unlike mRNA transfection, protein transduction does not require a transfection reagent, which is generally toxic to cells, so that TFs can be continuously added to the medium at a high concentration, enabling strong and continuous expression. However, their use has been hampered by the interference of PTDs with the function of TFs (Ye et al., 2002). In this study, we demonstrated that intracellular removal of PTD indeed restored the function of TFs using TEV protease as an example of this strategy. The activity of TEV protease was probably sufficient for processing most TFs, since quite a high level of exogenous Sox2 or Oct3/4 is known to be required for rescuing the repression of endogenous counterparts in ES cells. In future, it is conceivable that combination of PTD-TEVR-TFs introduced by protein transduction with TEV protease expressed by an RNA-based system (e.g., SeV) may achieve efficient cellular induction. In addition, this may reduce concern for any unexpected effect of expression of residual TFs (compared with all TFs being introduced by SeV), and may considerably reduce safety verification steps for clinical use.

In summary, we demonstrated that removal of PTD fused with Sox2 or Oct3/4 within ES cells restored protein function. This suggests that if PTD is removed from cells, directly delivered TF proteins, in general, may be able to exert substantially enhanced function than presently considered. This may enable induction of most cell types by protein transduction, and TEV protease may be a useful tool for this approach.

Funding

This work was supported in part by Grants-in-Aid for Scientific Research from the Ministry of Health, Labor, and Welfare of Japan.

Acknowledgments

We are grateful to Dr. Barbara Lee Smith Pierce (University of Maryland University College) for editorial work in the preparation of this manuscript.

References

Davis, R.L., Weintraub, H., Lassar, A.B., 1987. Expression of a single transfected cDNA converts fibroblasts to myoblasts. Cell 51, 987–1000.
Derossi, D., Calvet, S., Trembleau, A., Brunissen, A., Chassaing, G., Prochiantz, A., 1996. Cell internalization of the third helix of the Antennapedia homeodomain is receptor-independent. J. Biol. Chem. 271, 18188–18193.
Dougherty, W.G., Carrington, J.C., Cary, S.M., Parks, T.D., 1988. Biochemical and mutational analysis of a plant virus polyprotein cleavage site. EMBO J. 7, 1281–1287.
Feng, R., Desbordes, S.C., Xie, H., Tillo, E.S., Pixley, F., Stanley, E.R., Graf, T., 2008. PU.1 and C/EBPalpha/beta convert fibroblasts into macrophage-like cells. Proc. Natl. Acad. Sci. U.S.A. 105, 6057–6062.
Frankel, A.D., Pabo, C.O., 1988. Cellular uptake of the tat protein from human immunodeficiency virus. Cell 55, 1189–1193.
Hanna, J., Wernig, M., Markoulaki, S., Sun, C.W., Meissner, A., Cassady, J.P., Beard, C., Brambrink, T., Wu, L.C., Townes, T.M., Jaenisch, R., 2007. Treatment of sickle cell anemia mouse model with iPS cells generated from autologous skin. Science 318, 1920–1923.
Ieda, M., Fu, J.D., Delgado-Olguin, P., Vedantham, V., Hayashi, Y., Bruneau, B.G., Srivastava, D., 2010. Direct reprogramming of fibroblasts into functional cardiomyocytes by defined factors. Cell 142, 375–386.
Inoue, M., Tokusumi, Y., Ban, H., Kanaya, T., Tokusumi, T., Nagai, Y., Iida, A., Hasegawa, M., 2003. Nontransmissible virus-like particle formation by F-deficient sendai virus is temperature sensitive and reduced by mutations in M and HN proteins. J. Virol. 77, 3238–3246.
Kapust, R.B., Tozser, J., Fox, J.D., Anderson, D.E., Cherry, S., Copeland, T.D., Waugh, D.S., 2001. Tobacco etch virus protease: mechanism of autolysis and rational design of stable mutants with wild-type catalytic proficiency. Protein Eng 14, 993–1000.
Kapust, R.B., Waugh, D.S., 2000. Controlled intracellular processing of fusion proteins by TEV protease. Protein Expr Purif 19, 312–318.
Kim, D., Kim, C.H., Moon, J.I., Chung, Y.G., Chang, M.Y., Han, B.S., Ko, S., Yang, E., Cha, K.Y., Lanza, R., Kim, K.S., 2009. Generation of human induced pluripotent stem cells by direct delivery of reprogramming proteins. Cell Stem Cell 4, 472–476.
Li, H.O., Zhu, Y.F., Asakawa, M., Kuma, H., Hirata, T., Ueda, Y., Lee, Y.S., Fukumura, M., Iida, A., Kato, A., Nagai, Y., Hasegawa, M., 2000. A cytoplasmic RNA vector derived from nontransmissible Sendai virus with efficient gene transfer and expression. J. Virol. 74, 6564–6569.
Masui, S., Nakatake, Y., Toyooka, Y., Shimosato, D., Yagi, R., Takahashi, K., Okochi, H., Okuda, A., Matoba, R., Sharov, A.A., Ko, M.S., Niwa, H., 2007. Pluripotency governed by Sox2 via regulation of Oct3/4 expression in mouse embryonic stem cells. Nat. Cell Biol. 9, 625–635.
Matsushita, M., Tomizawa, K., Moriwaki, A., Li, S.T., Terada, H., Matsui, H., 2001. A high-efficiency protein transduction system demonstrating the role of PKA in long-lasting long-term potentiation. J. Neurosci. 21, 6000–6007.
Morita, S., Kojima, T., Kitamura, T., 2000. Plat-E: an efficient and stable system for transient packaging of retroviruses. Gene Ther. 7, 1063–1066.
Niwa, H., Miyazaki, J., Smith, A.G., 2000. Quantitative expression of Oct-3/4 defines differentiation, dedifferentiation or self-renewal of ES cells. Nat. Genet. 24, 372–376.
Okita, K., Ichisaka, T., Yamanaka, S., 2007. Generation of germline-competent induced pluripotent stem cells. Nature 448, 313–317.

Okita, K., Nakagawa, M., Hyenjong, H., Ichisaka, T., Yamanaka, S., 2008. Generation of mouse induced pluripotent stem cells without viral vectors. Science 322, 949–953.
Pauli, A., Althoff, F., Oliveira, R.A., Heidmann, S., Schuldiner, O., Lehner, C.F., Dickson, B.J., Nasmyth, K., 2008. Cell-type-specific TEV protease cleavage reveals cohesin functions in Drosophila neurons. Dev Cell 14, 239–251.
Phelan, A., Elliott, G., O'Hare, P., 1998. Intercellular delivery of functional p53 by the herpesvirus protein VP22. Nat. Biotechnol. 16, 440–443.
Rigaut, G., Shevchenko, A., Rutz, B., Wilm, M., Mann, M., Seraphin, B., 1999. A generic protein purification method for protein complex characterization and proteome exploration. Nat Biotechnol 17, 1030–1032.
Takahashi, K., Yamanaka, S., 2006. Induction of pluripotent stem cells from mouse embryonic and adult fibroblast cultures by defined factors. Cell 126, 663–676.
Takenobu, T., Tomizawa, K., Matsushita, M., Li, S.T., Moriwaki, A., Lu, Y.F., Matsui, H., 2002. Development of p53 protein transduction therapy using membrane-permeable peptides and the application to oral cancer cells. Mol. Cancer Ther. 1, 1043–1049.
Vierbuchen, T., Ostermeier, A., Pang, Z.P., Kokubu, Y., Sudhof, T.C., Wernig, M., 2010. Direct conversion of fibroblasts to functional neurons by defined factors. Nature 463, 1035–1041.
Warren, L., Manos, P.D., Ahfeldt, T., Loh, Y.H., Li, H., Lau, F., Ebina, W., Mandal, P.K., Smith, Z.D., Meissner, A., Daley, G.Q., Brack, A.S., Collins, J.J., Cowan, C., Schlaeger, T.M., Rossi, D.J., 2010. Highly efficient reprogramming to pluripotency and directed differentiation of human cells with synthetic modified mRNA. Cell Stem Cell 7, 618–630.
Wawersik, S., Evola, C., Whitman, M., 2005. Conditional BMP inhibition in Xenopus reveals stage-specific roles for BMPs in neural and neural crest induction. Dev Biol 277, 425–442.
Wender, P.A., Mitchell, D.J., Pattabiraman, K., Pelkey, E.T., Steinman, L., Rothbard, J.B., 2000. The design, synthesis, and evaluation of molecules that enable or enhance cellular uptake: peptoid molecular transporters. Proc. Natl. Acad. Sci. U.S.A. 97, 13003–13008.
Wernig, M., Zhao, J.P., Pruszak, J., Hedlund, E., Fu, D., Soldner, F., Broccoli, V., Constantine-Paton, M., Isacson, O., Jaenisch, R., 2008. Neurons derived from reprogrammed fibroblasts functionally integrate into the fetal brain and improve symptoms of rats with Parkinson's disease. Proc. Natl. Acad. Sci. U.S.A. 105, 5856–5861.
Wehr, M.C., Laage, R., Bolz, U., Fischer, T.M., Grunewald, S., Scheek, S., Bach, A., Nave, K.A., Rossner, M.J., 2006. Monitoring regulated protein-protein interactions using split TEV. Nat Methods 3, 985–993.
Ye, D., Xu, D., Singer, A.U., Juliano, R.L., 2002. Evaluation of strategies for the intracellular delivery of proteins. Pharm. Res. 19, 1302–1309.
Zhou, Q., Brown, J., Kanarek, A., Rajagopal, J., Melton, D.A., 2008. In vivo reprogramming of adult pancreatic exocrine cells to beta-cells. Nature 455, 627–632.

Journal of Reproduction and Development, Vol. 57, No. 5, 2011

—Original Article—

The *Dnmt3b* Splice Variant is Specifically Expressed in *In Vitro*-manipulated Blastocysts and Their Derivative ES Cells

Takuro HORII[1], Isao SUETAKE[2], Eikichi YANAGISAWA[1], Sumiyo MORITA[1], Mika KIMURA[1], Yasumitsu NAGAO[3], Hiroshi IMAI[4], Shoji TAJIMA[2] and Izuho HATADA[1]

[1]Laboratory of Genome Science, Biosignal Genome Resource Center, Institute for Molecular and Cellular Regulation, Gunma University, Gunma 371-8512, [2]Laboratory of Epigenetics, Institute for Protein Research, Osaka University, Osaka 565-0871, [3]Medical Research Center, Jichi Medical University, Tochigi 329-0498 and [4]Laboratory of Reproductive Biology, Graduate School of Agriculture, Kyoto University, Kyoto 606-8502, Japan

Abstract. Manipulation of preimplantation embryos *in vitro*, such as *in vitro* fertilization (IVF), *in vitro* culture (IVC), intracytoplasmic sperm injection (ICSI), somatic cell nuclear transfer (SCNT) and other assisted reproduction technologies (ART), has contributed to the development of infertility treatment and new animal reproduction methods. However, such embryos often exhibit abnormal DNA methylation patterns in imprinted genes and centromeric satellite repeats. These DNA methylation patterns are established and maintained by three DNA methyltransferases: Dnmt1, Dnmt3a and Dnmt3b. Dnmt3b is responsible for the creation of methylation patterns during the early stage of embryogenesis and consists of many alternative splice variants that affect methylation activity; nevertheless, the roles of these variants have not yet been identified. In this study, we found an alternatively spliced variant of *Dnmt3b* lacking exon 6 (*Dnmt3bΔ6*) that is specific to mouse IVC embryos. *Dnmt3bΔ6* also showed prominent expression in embryonic stem (ES) cells derived from *in vitro* manipulated embryos. Interestingly, IVC blastocysts were hypomethylated in centromeric satellite repeat regions that could be susceptible to methylation by Dnmt3b. *In vitro* methylation activity assays showed that Dnmt3bΔ6 had lower activity than normal Dnmt3b. Our findings suggest that Dnmt3bΔ6 could induce a hypomethylation status especially in *in vitro* manipulated embryos.

Key words: DNA methylation, Dnmt3b, *In vitro* culture

(J. Reprod. Dev. 57: 579–585, 2011)

The 5th position cytosine residues in CpG sequences are often methylated in vertebrate genomic DNA [1]. DNA methylation plays an essential role in the normal development of mammalian embryos by regulating gene expression through genomic imprinting, X chromosome inactivation and genomic stability [2–6]. In vertebrates, two types of DNA methyltransferase activity have been reported, the *de novo* and maintenance types. In mice, *de novo*-type DNA methylation activity creates gene-specific methylation patterns during the implantation stage of embryogenesis, while maintenance-type activity ensures clonal transmission of lineage-specific methylation patterns during replication. Dnmt1 is responsible for the latter activity. On the other hand, two DNA methyltransferases, Dnmt3a and Dnmt3b, are responsible for creation of methylation patterns during the early stages of embryogenesis [7, 8] and have been shown to possess *de novo*-type DNA methylation activity *in vitro* [9–12]. Recent studies have shown that Dnmts function in cooperation with each other to facilitate DNA methylation in both humans and mice [13–15].

In mice, Dnmt3b is the major *de novo* DNA methyltransferase in E (embryonic stage) 4.5–7.5 embryos, and its expression is downregulated after midgestation [8, 16]. Disruption of Dnmt3b results in embryonic lethality at E13.5 and hypomethylation of centromeric minor satellite repeats [8]. In humans, DNMT3B mutations have been shown to cause ICF (immunodeficiency, chromosomal instability, and facial anomalies) syndrome [8, 17, 18]. Dnmt3b contains a C-terminal catalytic domain and a N-terminal regulatory domain including the PWWP domain and consists of more than 16 alternative splice variants [7, 19–22]. Among these variants, both Dnmt3b1 and Dnmt3b2 contain all of the highly conserved motifs (I, IV, VI, VIII, IX and X) in their catalytic domains. In contrast, Dnmt3b3 and Dnmt3b6, lacking motifs VII and VIII and nine amino acids of motif IX [19], are catalytically inactive both *in vitro* [9] and *in vivo* [23]. On the other hand, the splicing variant of the regulatory domain, human DNMT3BΔ5 (the same variant as mouse Dnmt3bΔ6), which lacks exon 5 (exon 6) adjacent to the PWWP domain, was recently reported to be upregulated in cancer cell lines that often show hypomethylation in centromeric repeated sequences [24]. Gopalakrishnan *et al.* indicated that this splicing region is responsible for DNA binding activity [24]; however, the role of this region has not yet been fully investigated. Interestingly, forced expression of DNMT3BΔ5 results in hypomethylation of centromeric and pericentromeric repeated sequences [24]. Similarly, forced expression of human specific DNMT3B4, which lacks a catalytic domain, induced DNA demethylation on satellite 2 in pericentromeric DNA [25]. These reports indicate that Dnmt3b variants have complicated roles in maintenance of DNA methylation status.

As is generally known, *in vitro* embryo manipulation technologies such as IVC, ICSI and SCNT have contributed to the

Received: October 22, 2010
Accepted: April 27, 2011
Published online in J-STAGE: June 10, 2011

Correspondence: I Hatada (e-mail: hatada@gunma-u.ac.jp)

development of infertility treatments and animal reproduction techniques. However, it has been reported that *in vitro* manipulated embryos often show abnormal DNA methylation patterns in differentially methylated regions (DMRs) of imprinted genes [26–29]. Moreover, a growing number of reports suggest that embryo manipulation *in vitro* increases the risk of diseases caused by aberrant DNA methylation patterns, such as Angelman syndrome (AS) and Beckwith–Wiedemann syndrome (BWS) [30–34]. Nevertheless, the factor(s) that causes DNA methylation instability in *in vitro* manipulated embryos has not yet been identified. Hence, we initiated experiments on the basis of the expectation that Dnmt3bΔ6 is responsible for hypomethylation in *in vitro* manipulated embryos.

Materials and Methods

Animals

C57BL/6J mice (B6, JAX mice), CD1 mice (Charles River, Yokohama, Japan) and F344 rats (CLEA Japan, Tokyo, Japan) were used in this study. All animal experiments were conducted according to the guidelines of the Animal Care and Experimentation Committee of Gunma University, Showa Campus, Japan.

Embryo collection, culture and transfer

C57BL/6J females were superovulated by injection of 5 units of pregnant mare serum (PMSG, ASKA Pharmaceutical, Tokyo, Japan) followed by injection of 5 units of human chorionic gonadotropin 48 h later (hCG, ASKA Pharmaceutical). Females were bred to C57BL/6J males overnight. Approximately 24 h after hCG, the females were sacrificed, and fertilized embryos were collected from the oviducts. These embryos were cultured as IVC blastocysts to the blastocyst stage (114 h after hCG) in M16 medium. In contrast, the *in vivo*-developed blastocysts were collected from uteri 96 h after hCG. The methods used to produce parthenogenetic embryos [35] and SCNT embryos have been described previously [36]. Some of the IVC and *in vivo*-developed blastocysts were transferred to the uterine horns of pseudopregnant recipient females (CD1) 2.5 days postcoitus (dpc), and these embryos were harvested after 7 days (9.5 dpc).

Cell counting of blastocysts

Inner cell mass (ICM) and trophectoderm (TE) cell numbers of blastocysts were counted as previously reported [37].

Generation of ES cell lines

The methods used for generation of ES cell lines have been previously described [35, 38]. Briefly, blastocysts were transferred into gelatinized tissue culture wells (2–3 blastocysts per well of a 4-well multiplate, Nunc, Rochester, NY, USA) and cultured for 7 days in ES medium and DMEM (Gibco, Gland Island, NY, USA) containing 17.5% Knockout SR (Gibco) following standard procedures [39, 40]. After 7 days, ICM outgrowths were harvested in trypsin/EDTA (0.25%/1 mM, Gibco), disaggregated by mouth pipetting and plated onto gelatinized tissue culture wells in ES medium (passage 1). Clones morphologically resembling ES cells were then picked and disaggregated a second time. The cells were then expanded and passaged prior to freezing or use.

DNA isolation and methylation analysis

DNA was isolated from about 10 blastocysts in each pool. Bisulfite treatment was carried out using an EpiTect Bisulfite Kit (Qiagen, Hilden, Germany), according to the manufacturer's instructions. PCR amplification of major and minor satellite DNA was performed for each set of primers:

major satellite,
5'-AAATCTAGAAATGTTTATTGTAGGA-3' and
5'-TTCGGATCCTAAAATATATATTTCTCAT-3';
minor satellite,
5'-TATGGAAAATGATAAAAATTATATTG-3' and
5'-ATTATAACTCATTAATATACACTATTC-3'.

The amplification consisted of a total of 21 cycles at 94 C for 10 sec, 55 C for 30 sec and 72 C for 60 sec for the major satellite primers and a total of 26 cycles at 94 C for 10 sec, 58 C for 30 sec and 72 C for 60 sec for the minor satellite primers using a GeneAmp PCR System 9700 (Applied Biosystems, Foster City, CA, USA). PCR products derived from 3 independent pools were subcloned into a TA cloning vector (pCR 2.1, Invitrogen). Positive clones for each sample were sequenced using the BigDye terminator method (ABI PRISM 3100, Applied Biosystems).

RNA extraction and reverse transcriptase-polymerase chain reaction (RT-PCR)

Total RNA was purified from embryos and nonhuman tissue using TRIzol reagent (Invitrogen, Carlsbad, CA, USA). Total RNA was obtained from human tissue using Human Total RNA Master Panel II (BD Biosciences, San Jose, CA, USA). Purified RNA from 50 blastocysts or 1 μg of purified RNA from postimplantation embryos and tissues was reverse transcribed using Superscript II (TaKaRa, Otsu, Japan) and Oligo(dT)$_{12-18}$ (TaKaRa) in a total volume of 20 μl. The mRNA expression level of each *Dnmt3bs* was determined by PCR using LA Taq HS DNA polymerase (Takara) and the primer sets shown in Table 1. PCR products were separated electrophoretically on a 2.5% agarose gel. For densitometry, the Quantity One software (Bio-Rad, Hercules, CA, USA) was used according to the manufacturer's instructions, and the expression ratios of –exon 6/+exon 6 (–exon 5/+exon 5) were calculated. Quantitative real-time RT-PCR for *Dnmt3b* was also carried out as previously reported [38].

Identification of Dnmt3bΔ6 splice variants

Mouse *Dnmt3b* cDNA was amplified from SCNT ES cells using primers S5 and AS3 (Table 1). PCR products were subcloned into the TA cloning vector (pCR 2.1; Invitrogen). RT-PCR primers for the *Dnmt3b* splice sites (Table 1) were used to identify splice variants. To confirm the variant sequences, the clones were sequenced using the BigDye terminator method (ABI PRISM 3100, Applied Biosystems).

Purification of recombinant Dnmt3b

Recombinant His-tagged Dnmt3b protein was produced in sf9 cells using the baculovirus expression system (Invitrogen) as described previously [41]. The ATG coding initiation methionines

Table 1. Sequences of the primers used for PCR amplification

Gene name		Sequence	Product size	Target
Mouse				
Dnmt3b	S1	gggaacttcagtgaccagtcctc	565 bp	Exon 6
	AS1	ccacctgtgtggtatcca		
	S2	ctggagagtcactggaggaccagctgaagc	290 bp	Exon 11
	AS2	ctctcctcatcctcccctcggtccttc		
	S3	acaaccgtccattcttctgg	391 bp	Catalytic region
	AS3	acgtccgtgtagtgagcaggga		
	S4	ctttcaggaaacaatgaaggga	2716 bp	Full length
	AS4	gctgaggtacagtgatgtga		
	S5	aaagcccggcttctcggaga	2002 bp	Dnmt3bΔ6 variants
	AS3	acgtccgtgtagtgagcaggga		
Gapdh	S	aatgcatcctgcaccaccaa	106 bp	
	AS	gtggcagtgatggcatggac		
Rat				
Dnmt3b	S	gtgaagcggatgatggagat	458 bp	Exon 6
	AS	ctttccccacacaaggtcac		
Gapdh	S	aatgcatcctgcaccaccaa	106 bp	
	AS	gtggcagtgatggcatggac		
Human				
DNMT3B	S	ccaggactcgttcagaaagc	237 bp	Exon 5
	AS	cgtctgtgaggtcgatggta		
GAPDH	S	aatgcctcctgcaccaccaa	106 bp	
	AS	gtggcagtgatggcatggac		

of mouse *Dnmt3b1Δ6* and *Dnmt3b1* were directly ligated using a BamH1 linker without any spacer sequence and then subcloned into the BamH1 site of the multicloning site of the pFAST-BACHTb vector (Invitrogen). Recombinant baculoviruses were constructed according to the manufacturer's instructions, and the viruses were amplified by three rounds of infection to obtain a high-titer baculovirus stock. Sf9 cells were maintained in Grace's medium containing 10% (v/v) fetal bovine serum at 27 C. The recombinant baculoviruses harboring Dnmt3b1Δ6 and Dnmt3b1 were infected into 5×10^8 sf9 cells at an M.O.I. (multiplicity of infection) of 2. After infection, the cells were incubated for 16 or 66 h and then harvested. Purification of His-Dnmt3b was carried out as described previously [41].

DNA methylation activity assay

The DNA methylation activity was determined as described elsewhere [9]. In brief, 50 ng (about 0.5 pmol) of purified Dnmt3b, 0.1 mg of dGdC and 133 pmol (2.0 μCi and 5.3 μM) of [^{3}H]-*S*-adenosyl-L-methionine (AdoMet) (15Ci/mmol, GE Healthcare, Uppsala, Sweden) were added to 25 μl of the reaction buffer (2.7 M glycerol, 5 mM EDTA, 0.2 mM DTT, 40–160 mM NaCl and 20 mM Tris-Hcl at pH 7.4). After a 1-h incubation, the reaction was terminated with 1.5 mM nonradioactive AdoMet. The mixtures were then incubated with 0.1 μg of proteinase K (Nacalai Tesque, Kyoto, Japan) at 50 C for 20 min, and the level of radioactivity was then determined as described previously [42].

Statistical analysis

QUMA (QUantification tool for Methylation Analysis, http://quma.cdb.riken.jp/) was used to statistically analyze the bisulfite sequencing of CpG methylation. The entire set of CpG sites was evaluated with the Mann-Whitney *U*-test. The Student's *t*-test was used for gene expression analysis and cell number analysis. Data are shown as means and standard deviations (SD). A P-value of <0.05 was considered significant.

Results and Discussion

Dnmt3bΔ6 expression in embryos and ES cell lines

A lot of reports have suggested that *in vitro* manipulation causes aberrant DNA methylation patterns (mostly hypomethylation) in the DMRs of imprinted genes in preimplantation embryos, whereas there have been few reports about the methylation patterns in the satellite repeat regions in these embryos. Therefore, we first exam-

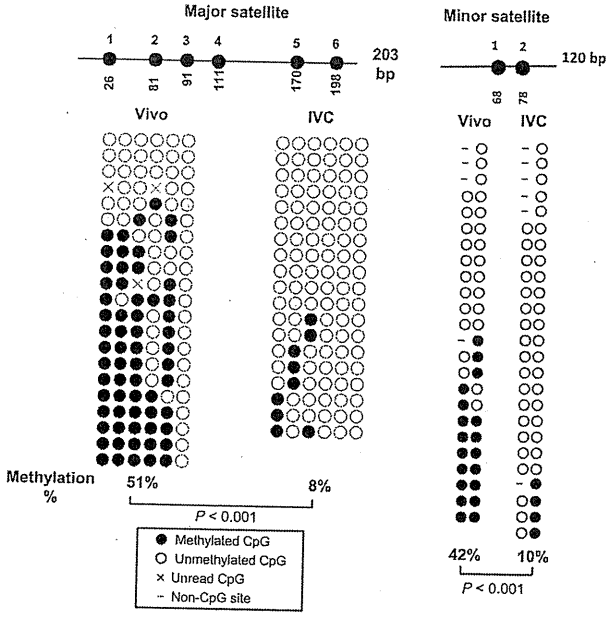

Fig. 1. DNA methylation status of centromeric repeat regions in blastocysts. Hypomethylation of major and minor satellite repeats was observed in *in vitro*-cultured blastocysts (IVC) relative to *in vivo*-developed blastocysts (Vivo).

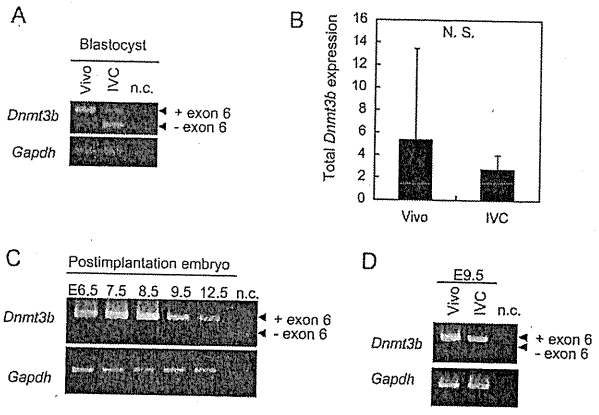

Fig. 2. *Dnmt3bΔ6* (exon 6 splice form) expression in mouse embryos. A: *Dnmt3b* containing exon 6 was the major transcript in blastocysts developed *in vivo* (Vivo), whereas both the spliced and unspliced forms were present in *in vitro*-cultured blastocysts (IVC). n.c., negative control. B: Total *Dnmt3b* expression was not significantly different (N. S.) between Vivo and IVC blastocysts. C: *Dnmt3bΔ6* was detected at very low levels in embryos postimplantation. D: *Dnmt3bΔ6* expression was not detectable in E9.5 fetuses derived from IVC embryos, indicating that the spliced form is expressed in undifferentiated cells and is then repressed during differentiation. n.c., negative control.

Table 2. Means of inner cell mass (ICM), trophectoderm (TE) and total cell number of blastocysts

Blastocysts	Cell number (mean ± SD) Total	ICM	TE	
In vivo (96 h)	43.3 ± 7.4	12.1 ± 2.8	31.2 ± 6.3	(N = 11)
IVC (114 h)	40.0 ± 8.6	12.0 ± 4.4	28.0 ± 6.1	(N = 10)

ined the DNA methylation statuses of these regions, and we found that IVC blastocysts are aberrantly hypomethylated relative to control *in vivo*-derived blastocysts (Fig. 1). Dnmt3b is the primary *de novo* DNA methyltransferase that methylates satellite repeats, especially the centromeric minor satellite repeats [8]. We hypothesized that the abnormal hypomethylation could be caused by the altered expression of specific *Dnmt3b* splicing variants in *in vitro*-manipulated embryos. To determine whether distinct *Dnmt3b* splicing variants were specifically expressed in preimplantation embryos (blastocyst stage), we prepared IVC blastocysts (114 h after hCG) and *in vivo*-developed blastocysts (96 h after hCG). At these times, ICM, TE and total cell numbers were not significantly different between IVC and *in vivo* developed blastocysts, indicating that both embryos were at the same developmental stage (Table 2). RT-PCR using a primer set that recognizes exon 6 splicing variants showed that *Dnmt3bΔ6* was more highly expressed in IVC blastocysts than *in vivo*-developed blastocyst controls (Fig. 2A), although the total Dnmt3b expression levels were not significantly different (Fig. 2B). In general, Dnmt3b is the major *de novo* DNA methyltransferase in E4.5–7.5 embryos, and its expression is down-regulated after midgestation [8, 16]. Our data agree with the findings of these reports (Fig. 2C). In addition, *Dnmt3bΔ6* expression was not detected in *in vivo* embryos during postimplantation development (Fig. 2C). Similarly, *Dnmt3bΔ6* expression was not detectable in E9.5 embryos that were produced by transplantation of IVC blastocysts into pseudopregnant females (Fig. 2D). These results indicate that *Dnmt3bΔ6* is specifically expressed in preimplantation blastocysts. High levels of *Dnmt3bΔ6* were also detected in undifferentiated ES cells generated from *in vitro* manipulated embryos, such as those generated by IVC (Fig. 3A), by parthenogenetic methods or from SCNT blastocysts (Fig. 3B). Thus, *Dnmt3bΔ6* is specifically expressed in undifferentiated cell types such as preimplantation embryos manipulated *in vitro* and their derivative ES cells.

Identification of Dnmt3bΔ6 splice variants

At least 16 *Dnmt3b* variants have been described in mice [22]; therefore, we performed PCR analysis using a primer set that amplified exon 6-deleted forms, and the PCR products were subcloned into a TA cloning vector. Each clone was characterized by

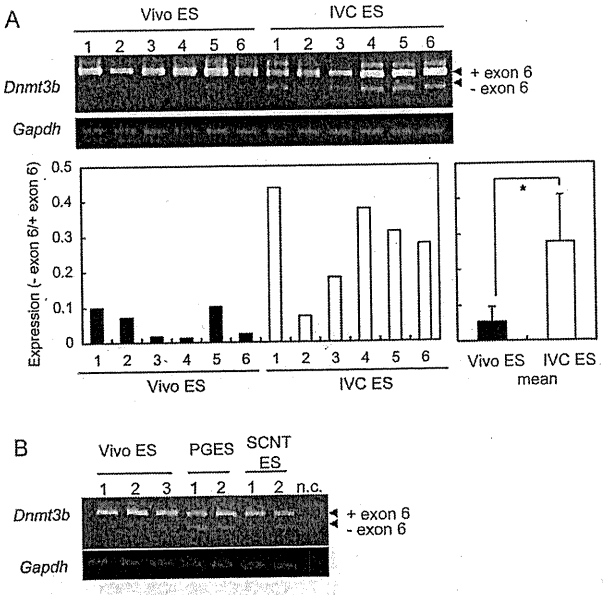

Fig. 3. *Dnmt3bΔ6* (exon 6 splice form) expression in mouse ES cells. A: *Dnmt3bΔ6* was more highly expressed in IVC embryo-derived ES cells (IVC ES) than in ES cells generated from *in vivo*-developed blastocysts (Vivo ES). * $P<0.05$. B: *Dnmt3bΔ6* was more highly expressed in ES cells that had been generated from *in vitro*-manipulated embryos, such as those generated by parthenogenesis (PG) and somatic cell nuclear transfer (SCNT). n.c., negative control.

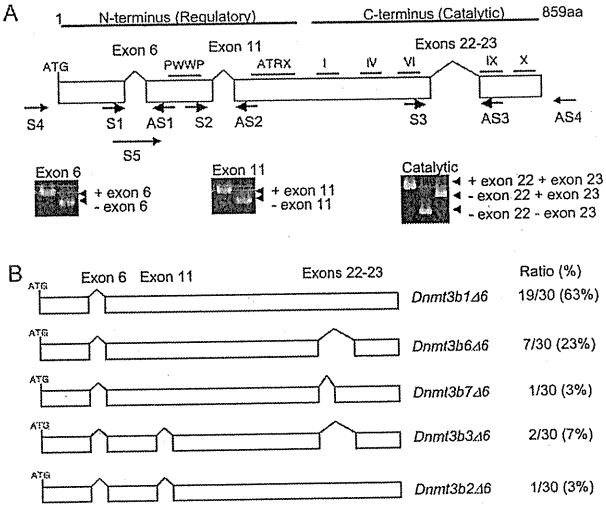

Fig. 4. Identification of mouse *Dnmt3bΔ6* splice variants. A: *Upper panel*: map of *Dnmt3b* mRNA showing the positions of conserved domains. *Arrows*: locations of the RT-PCR primers used in this study. *Lower panel*: RT-PCR analysis of cloned alternative splicing variants identified those lacking exons 6, 11 and 22–23. B: Organization of the *Dnmt3bΔ6* mRNA species present in SCNT ES cells. The PCR products amplified from *Dnmt3bΔ6* cDNA were subcloned into a TA cloning vector, and each clone was characterized by sequencing. The most common form of *Dnmt3b1Δ6* identified was *Dnmt3b1Δ6* (63%), while the second most common form was *Dnmt3b6Δ6* (23%).

RT-PCR and sequencing to identify individual variants. From these analyses, five variants lacking exon 6 were identified. The most prevalent form identified was *Dnmt3b1Δ6* (63%), which only lacked exon 6, and the second most common form was *Dnmt3b6Δ6* (23%), which lacked exon 6 and exons 22–23 of the catalytic domain (Fig. 4A and B).

DNA methylation activity of purified Dnmt3bΔ6

To determine the DNA methylation activity of Dnmt3b1Δ6 *in vitro*, sf9 cells were infected with recombinant baculoviruses encoding Dnmt3b1 and Dnmt3b1Δ6, and recombinant Dnmt3b1 and Dnmt3b1Δ6 were then purified (Fig. 5A and B). Dnmt3b1Δ6 demonstrated DNA methylation activity, although it showed lower activity than the control Dnmt3b1 (Fig. 5C). The second major variant, Dnmt3b6Δ6, which lacks the catalytic domain, was not examined; however, Dnmt3b6Δ6 is not expected to possess methylation activity, as all the other mouse Dnmt3b variants without the catalytic domain (e.g., Dnmt3b3) do not possess methylation activity. Thus, we concluded that there would be insufficient methylation activity in cells, such as IVC blastocysts, in which the dominant Dnmt3b form is Dnmt3bΔ6.

Tissue- and species-specific expression of Dnmt3bΔ6

According to the NCBI (National Center for Biotechnology Information) database, the exon 6 region is highly conserved among mice, rats and humans. To determine the expression pattern of *Dnmt3bΔ6* in these species, RT-PCR was performed using exon 6-specific primer sets. In mice, only low levels of *Dnmt3bΔ6* expression were observed in all tissues except for skeletal muscle (Fig. 6A). A very low level of *Dnmt3bΔ6* expression was also seen in rat tissues (Fig. 6B). Human *DNMT3B* lacks one noncoding exon at its 5'-end; therefore, the region equivalent to exon 6 in mouse *Dnmt3b* is exon 5 in human *DNMT3B*. Interestingly, the highest levels of human *DNMT3B* lacking exon 5 (*DNMT3BΔ5*) expression were observed in both the adult and fetal brain (Fig. 6 C). DNMT3B is reported to be necessary for nerve growth factor-mediated differentiation [43], and the DNMT3B mutations that occur in ICF syndrome lead to altered epigenetic modifications and aberrant expression of genes regulating neurogenesis [44]. This variant is thus proposed to be necessary for the development and maintenance of neural function in humans. In contrast, only a low level of *Dnmt3bΔ6* expression was observed in mouse and rat brains. The reason for the difference between human and rodent *Dnmt3b* expression is presently unclear. Further studies will be required to elucidate the specific roles of Dnmt3bΔ6 in neural development.

Dnmt3bΔ6 and centromeric hypomethylation

In vitro manipulated embryos often exhibit abnormal methylation patterns in genomic imprinting regions and centromeric repeats. In this study, we have shown the first evidence that *Dnmt3bΔ6*, which is highly expressed in *in vitro* manipulated

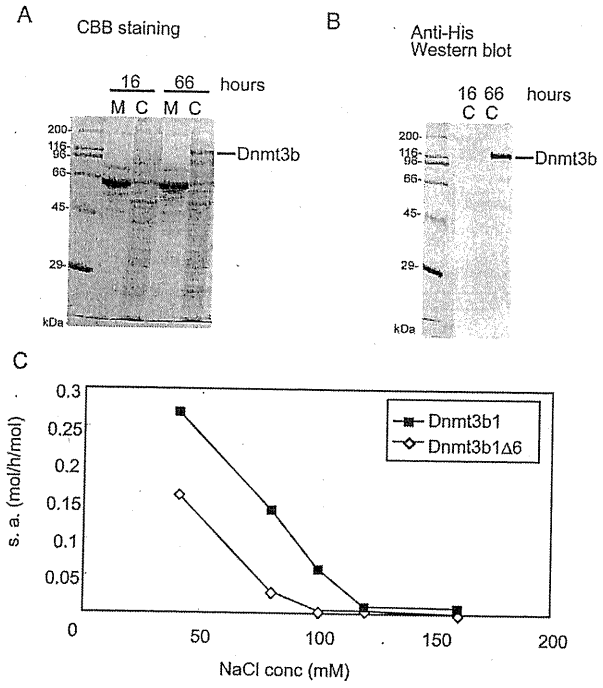

Fig. 5. *De novo* methylation activity of purified Dnmt3bΔ6. A: Recombinant baculoviruses encoding Dnmt3bΔ6 were generated and used to infect sf9 cells. Samples obtained 16 and 66 h after infection were subjected to SDS-PAGE and then stained with CBB. M, medium fraction; C, cell fraction. B: Purified protein was blotted with an anti-His antibody. C: The DNA methylation activity [specific activity (s.a.) in mol/h/mol] of Dnmt3b1Δ6 and Dnmt3b1 was titrated with NaCl.

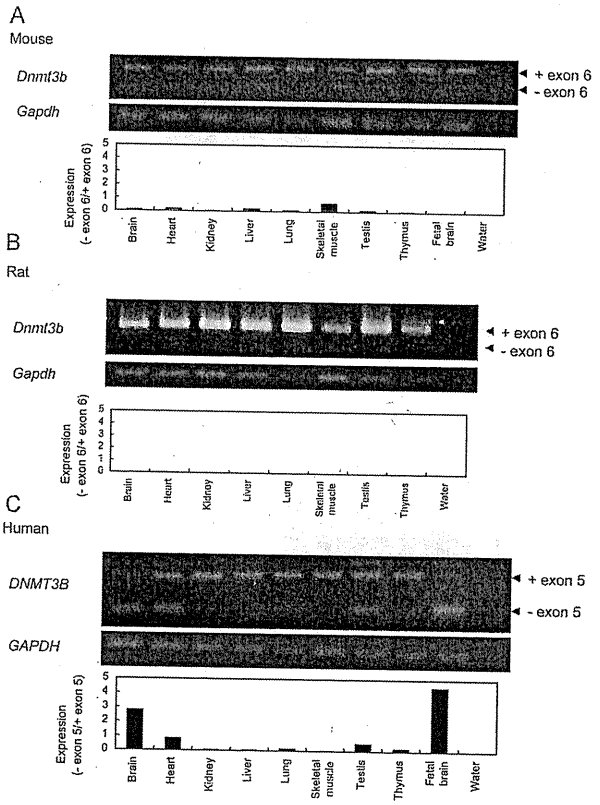

Fig. 6. *Dnmt3bΔ6* (*DNMT3BΔ5*) expression in various tissues. *Dnmt3b* containing exon 6 was the abundantly expressed variant in mouse tissues (A) and in rat tissues (B). C: In humans, *DNMT3B* lacking exon 5 was the predominant form in adult and fetal brains.

embryos, may be involved in abnormal DNA methylation. *Dnmt3bΔ6* (*DNMT3BΔ5*) is also overexpressed in human cancer cell lines [24] that often exhibit global hypomethylation, where it primarily affects repetitive regions of the genome, such as the centromeric and pericentromeric regions [45]. Notably, ectopic overexpression of DNMT3B3Δ5 resulted in repetitive element hypomethylation in cancer cells [24]. Thus, Dnmt3bΔ6 could be involved in DNA hypomethylation, especially in the centromeric and pericentromeric satellite repeat region in early embryos. After fertilization, the embryonic genome, including the centromeric satellite repeats, becomes demethylated, and these methylation levels are maintained during preimplantation development [46, 47]. Even blastocysts that develop *in vivo* exhibit low levels of *Dnmt3bΔ6* expression, implying that Dnmt3bΔ6 is essential for demethylation or maintenance of the methylation status of centromeric satellite repeats. Consistent with this hypothesis, excessive expression of *Dnmt3bΔ6* in IVC embryos may induce abnormal DNA methylation. Thus, the expression pattern of Dnmt3bΔ6 and other Dnmt3b variants seems to be precisely regulated at the preimplantation stage. Although we do not have information about how *Dnmt3b* splicing is regulated, small nuclear ribonucleoprotein particles (snRNPs) and their mediator SF2/ASF [48, 49] are likely candidates.

In vitro embryo manipulation technologies have contributed to the development of infertility treatments and new animal reproduction strategies. However, *in vitro* embryo manipulation increases the risk of epigenetic abnormalities, a crucial problem that remains to be solved. Our findings regarding Dnmt3bΔ6 expression may provide clues as to why epigenetic abnormalities occur in embryos manipulated *in vitro*.

Acknowledgments

We thank Dr S Ikeda (Kyoto University) for his technical advice regarding sf9 cell culture and cell counting of blastocysts. This study was supported in part by grants from the Japanese Science and Technology Agency; the National Institute of Biomedical Innovation; the Ministry of Education, Culture, Sports, Science and Technology of Japan; the Takeda Science Foundation; joint research program of the Institute for Molecular and Cellular Regulation, Gunma University; and the Ministry of Health, Labour, and Welfare of Japan.

References

1. **Antequera F, Bird A.** CpG islands in DNA methylation. *In*: Jost JP, Saluz HP (eds.), Molecular Biology and Biological Significance. Basel: Birkhauser Verlag; 1993: 169–185.
2. **Jaenisch R.** DNA methylation and imprinting: why bother? *Trends Genet* 1997; 13: 323–329.
3. **Jones P, Gonzalgo M.** Altered DNA methylation and genome instability: a new pathway to cancer? *Proc Natl Acad Sci USA* 1997; 94: 2103–2105.
4. **Robertson KD, Wolffe AP.** DNA methylation in health and disease. *Nat Rev Genet* 2000; 1: 11–19.
5. **Surani MA.** Imprinting and the initiation of gene silencing in the germline. *Cell* 1998; 93: 309–312.
6. **Monk M.** Changes in DNA methylation during mouse embryonic development in relation to X-chromosome activity and imprinting. *Phil Trans R Soc Lond* 1990; 326: 299–312.
7. **Okano M, Xie S, Li E.** Cloning and characterization of a family of novel mammalian DNA (cytosine-5) methyltransferases. *Nat Genet* 1998; 19: 219–220.
8. **Okano M, Bell DW, Haber DA, Li E.** DNA methyltransferases Dnmt3a and Dnmt3b are essential for *de novo* methylation and mammalian development. *Cell* 1999; 99: 247–257.
9. **Aoki A, Suetake I, Miyagawa J, Fujio T, Chijiwa T, Sasaki H, Tajima S.** Enzymatic properties of *de novo*-type mouse DNA (cytosine-5) methyltransferases. *Nucleic Acids Res* 2001; 29: 3506–3512.
10. **Gowher H, Jeltsch A.** Enzymatic properties of recombinant Dnmt3a DNA methyltransferase from mouse: The enzyme modifies DNA in a non-processive manner and also methylates non-CpG sites. *J Mol Biol* 2001; 309: 1201–1208.
11. **Lin IG, Han L, Taghva A, O'Brien LE, Hsieh CL.** Murine de novo methyltransferase Dnmt3a demonstrates strand asymmetry and site preference in the methylation of DNA *in vitro*. *Mol Cell Biol* 2002; 22: 704–723.
12. **Yokochi T, Robertson KD.** Preferential methylation of unmethylated DNA by mammalian *de novo* DNA methyltranasferase Dnmt3a. *J Biol Chem* 2002; 277: 11735–11745.
13. **Liang G, Chan M, Tomigahara Y, Tsai YC, Gonzales FA, Li E, Laird PW, Jones PA.** Cooperativity between DNA methyltransferases in the maintenance methylation of repetitive elements. *Mol Cell Biol* 2002; 22: 480–491.
14. **Rhee I, Bachman KE, Park BH, Jair KW, Yen RW, Schuebel KE, Cui H, Feinberg AP, Lengauer C, Kinzler KW, Baylin SB, Vogelstein B.** DNMT1 and DNMT3b cooperate to silence genes in human cancer cells. *Nature* 2002; 416: 552–556.
15. **Kim GD, Ni J, Kelesoglu N, Roberts RJ, Pradhan S.** Co-operation and communication between the human maintenance and *de novo* DNA (cytosine-5) methyltransferases. *EMBO J* 2002; 21: 4183–4195.
16. **Watanabe D, Suetake I, Tada T, Tajima S.** Stage- and cell-specific expression of Dnmt3a and Dnmt3b during embryogenesis. *Mech Dev* 2002; 118: 187–190.
17. **Hansen RS, Wijmenga C, Luo P, Stanek AM, Canfield TK, Weemaes CM, Gartler SM.** The DNMT3B DNA methyltransferase gene is mutated in ICF immunodeficiency syndrome. *Proc Natl Acad Sci USA* 1999; 96: 14412–14417.
18. **Xu GL, Bestor TH, Bourc'his D, Hsieh C, Tommerup N, Bugge M, Hulten M, Qu X, Russo JJ, Viegas-Pequignot E.** Chromosome instability and immunodeficiency syndrome caused by mutations in a DNA methyltransferase gene. *Nature* 1999; 402: 187–190.
19. **Robertson KD, Uzvolgy E, Liang G, Talmadge C, Sumegi J, Gonzales FA, Jones PA.** The human DNA methyltransferases (DNMTs) 1, 3a and 3b: coordinate mRNA expression in normal tissues and overexpression in tumors. *Nucleic Acids Res* 1999; 27: 2291–2298.
20. **Xie S, Wang Z, Okano M, Nogami M, Li Y, He WW, Okumura K, Li E.** Cloning, expression and chromosome locations of the human DNMT3 gene family. *Gene* 1999; 236: 87–95.
21. **Chen T, Ueda Y, Xie S, Li E.** A novel Dnmt3a isoform produced from an alternative promoter localizes to euchromatin and its expression correlates with active *de novo* methylation. *J Biol Chem* 2002; 277: 38746–38754.
22. **Weisenberger DJ, Velicescu M, Cheng JC, Gonzales FA, Liang G, Jones PA.** Role of the DNA methyltransferase variant DNMT3b3 in DNA methylation. *Mol Cancer Res* 2004; 2: 62–72.
23. **Chen T, Ueda Y, Dodge JE, Wang Z, Li E.** Establishment and maintenance of genomic methylation patterns in mouse embryonic stem cells by Dnmt3a and Dnmt3b. *Mol Cell Biol* 2003; 23: 5594–5605.
24. **Gopalakrishnan S, Van Emburgh BO, Shan J, Su Z, Fields CR, Vieweg J, Hamazaki T, Schwartz PH, Terada N, Robertson KD.** A novel DNMT3B splice variant expressed in tumor and pluripotent cells modulates genomic DNA methylation patterns and displays altered DNA binding. *Mol Cancer Res* 2009; 7: 1622–1634.
25. **Saito Y, Kanai Y, Sakamoto M, Saito H, Ishii H, Hirohashi S.** Overexpression of a splice variant of DNA methyltransferase 3b, DNMT3b4, associated with DNA hypomethylation on pericentromeric satellite regions during human hepatocarcinogenesis. *Proc Natl Acad Sci USA* 2002; 99: 10060–10065.
26. **Doherty AS, Mann MR, Tremblay KD, Bartolomei MS, Schultz RM.** Differential effects of culture on imprinted *H19* expression in the preimplantation mouse embryo. *Biol Reprod* 2000; 62: 1526–1535.
27. **Khosla S, DeanW, Brown D, ReikW, Feil R.** Culture of preimplantation mouse embryos affects fetal development and the expression of imprinted gene. *Biol Reprod* 2001; 64: 918–926.
28. **Li T, Vu TH, Ulaner GA, Littman E, Ling JQ, Chen HL, Hu JF, Behr B, Giudice L, Hoffman AR.** IVF results in *de novo* DNA methylation and histone methylation at an *Igf2-H19* imprinting epigenetic switch. *Mol Hum Reprod* 2005; 11: 631–640.
29. **Zaitseva I, Zaitsev S, Alenina N, Bader M, Krivokharchenko A.** Dynamics of DNA-demethylation in early mouse and rat embryos developed *in vivo* and *in vitro*. *Mol Reprod Dev* 2007; 74: 1255–1261.
30. **Cox GF, Burger J, Lip V, Mau UA, Sperling K, Wu BL, Horsthemke B.** Intracytoplasmic sperm injection may increase the risk of imprinting defects. *Am J Hum Genet* 2002; 71: 162–164.
31. **DeBaun MR, Niemitz EL, Feinberg AP.** Association of *in vitro* fertilization with Beckwith-Wiedemann syndrome and epigenetic alterations of LIT1 and H19. *Am J Hum Genet* 2003; 72: 156–160.
32. **Gicquel C, Gaston V, Mandelbaum J, Siffroi JP, Flahault A, Le Bouc Y.** *In vitro* fertilization may increase the risk of Beckwith-Wiedemann syndrome related to the abnormal imprinting of the KCN1OT gene. *Am J Hum Genet* 2003; 72: 1338–1341.
33. **Maher ER, Brueton LA, Bowdin SC, Luharia A, Cooper W, Cole TR, Macdonald F, Sampson JR, Barratt C, Reik W, Hawkins MM.** Beckwith-Wiedemann syndrome and assisted reproduction technology (ART). *J Med Genet* 2003; 40: 62–64.
34. **Orstavik KH, Eiklid K, van der Hagen CB, Spetalen S, Kierulf K, Skjeldal O, Buiting K.** Another case of imprinting defect in a girl with Angelman syndrome who was conceived by intracytoplasmic semen injection. *Am J Hum Genet* 2003; 72: 218–219.
35. **Horii T, Kimura M, Morita S, Nagao Y, Hatada I.** Loss of genomic imprinting in mouse parthenogenetic embryonic stem cells. *Stem Cells* 2008; 26: 79–88.
36. **Ogura A, Inoue K, Takano K, Wakayama T, Yanagimachi R.** Birth of mice after nuclear transfer by electrofusion using tail tip cells. *Mol Reprod Dev* 2000; 57: 55–59.
37. **Thouas GA, Korfiatis NA, French AJ, Jones GM, Trounson AO.** Simplified technique for differential staining of inner cell mass and trophectoderm cells of mouse and bovine blastocysts. *Reprod Biomed Online* 2001; 3: 25–29.
38. **Horii T, Yanagisawa E, Kimura M, Morita S, Hatada I.** Epigenetic differences between embryonic stem cells generated from blastocysts developed *in vitro* and *in vivo*. *Cell Reprogram* 2010; 12: 551–563.
39. **Robertson EJ.** Embryo derived stem cell lines. *In*: Robertson EJ (ed.), Teratocarcinomas and Embryonic Stem Cells: A Practical Approach. Oxford: IRL Press; 1987: 71–112.
40. **Horii T, Nagao Y, Tokunaga T, Imai H.** Serum-free culture of murine primordial germ cells and embryonic germ cells. *Theriogenology* 2003; 59: 1257–1264.
41. **Suetake I, Miyazaki J, Murakami C, Takeshima H, Tajima S.** Distinct enzymatic properties of recombinant mouse DNA methyltransferases Dnmt3a and Dnmt3b. *J Biochem* 2003; 133: 737–744.
42. **Kimura H, Suetake I, Tajima S.** Xenopus maintenance-type DNA methyltransferase is accumulated in and translocated into germinal vesicles of oocytes. *J Biochem* 1999; 125: 1175–1182.
43. **Bai S, Ghoshal K, Datta J, Majumder S, Yoon SO, Jacob ST.** DNA methyltransferase 3b regulates nerve growth factor-induced differentiation of PC12 cells by recruiting histone deacetylase 2. *Mol Cell Biol* 2005; 25: 751–766.
44. **Jin B, Tao Q, Peng J, Soo HM, Wu W, Ying J, Fields CR, Delmas AL, Liu X, Qiu J, Robertson KD.** DNA methyltransferase 3B (DNMT3B) mutations in ICF syndrome lead to altered epigenetic modifications and aberrant expression of genes regulating development, neurogenesis and immune function. *Hum Mol Genet* 2008; 17: 690–709.
45. **Jones PA, Baylin SB.** The fundamental role of epigenetic events in cancer. *Nature Rev Genet* 2002; 3: 415–428.
46. **Kim SH, Kang YK, Koo DB, Kang MJ, Moon SJ, Lee KK, Han YM.** Differential DNA methylation reprogramming of various repetitive sequences in mouse preimplantation embryos. *Biochem Biophys Res Commun* 2004; 324: 58–63.
47. **Fernandez-Gonzalez R, Ramirez MA, Bilbao A, De Fonseca FR, Gutierrez-Adan A.** Suboptimal *in vitro* culture conditions: an epigenetic origin of long-term health effects. *Mol Reprod Dev* 2007; 74: 1149–1156.
48. **Krainer AR, Conway GC, Kozak D.** Purification and characterization of pre-mRNA splicing factor SF2 from HeLa cells. *Genes Dev* 1990 ; 4: 1158–1171.
49. **Krainer AR, Conway GC, Kozak D.** The essential pre-mRNA splicing factor SF2 influences 5' splice site selection by activating proximal sites. *Cell* 1990; 62: 35–42.

17

Differentiation of Cancer Stem Cells

Taro Yamashita, Masao Honda and Shuichi Kaneko
Department of Gastroenterology,
Kanazawa University Hospital Kanazawa, Ishikawa,
Japan

1. Introduction

Tumors originally develop from normal cells that acquire the ability to grow aberrantly and metastasize to distant organs (Hanahan and Weinberg, 2000). These malignant transformations are considered to be induced by the accumulation of multiple genetic/epigenetic changes (Yamashita et al., 2008b). Although considered monoclonal in origin, cancer is composed of heterogeneous cell populations. This heterogeneity is traditionally explained by the clonal evolution of cancer cells through a series of stochastic genetic events (clonal evolution model) (Fialkow, 1976; Nowell, 1976). In contrast, cancer cells and stem cells have similar capabilities with respect to self-renewal, limitless division, and the generation of heterogeneous cell populations. Recent evidence suggests that tumor cells possess stem cell features (cancer stem cells) to self-renew and give rise to relatively differentiated cells through asymmetric division, thereby forming heterogeneous populations (cancer stem cell model) (Clarke et al., 2006; Jordan et al., 2006). Accumulating evidence supports the notion that cancer stem cells can generate tumors more efficiently in immunodeficient mice than non-cancer stem cells in hematological malignancies and in various solid tumors (Al-Hajj et al., 2003; Bonnet and Dick, 1997; O'Brien et al., 2007; Ricci-Vitiani et al., 2007; Singh et al., 2004).

Cancer stem cells are considered to be resistant to chemotherapy and radiotherapy, which might be associated with the recurrence of the tumor after treatment (Boman and Huang, 2008; Dean et al., 2005; Diehn et al., 2009; Zou, 2008). These findings have led to the proposal of "destemming" cancer stem cells (Hill and Perris, 2007) in order to induce their differentiation into non-cancer stem cells or to eradicate cancer stem cells by inhibiting the signaling pathways responsible for their self-renewal. Recent studies have supported this proposal and suggest the utility of several factors to induce the differentiation of cancer stem cells and facilitate tumor eradication; however, it is still debatable whether the simple differentiation of cancer stem cells effectively eradicates tumors. Here, we summarize current knowledge on the differentiation of cancer stem cells and discuss the utility and limitation of differentiation therapy to eliminate cancer.

2. Cancer stem cell system

The consensus definition of a cancer stem cell is a cell within a tumor that possesses the capacity to self-renew and to generate the heterogeneous lineages of cancer cells that

comprise the tumor, as proposed by the AACR workshop in 2006 (Clarke et al., 2006). Thus, cancer stem cells can only be defined experimentally and their self-renewal ability is generally evaluated by the capacity of serially transplanted cells in immunodeficient mice. A cancer stem cell may give rise to one or two daughter cells that have essentially the same ability to replicate and generate differentiated non-cancer stem cells (Fig. 1 upper and lower left panels).

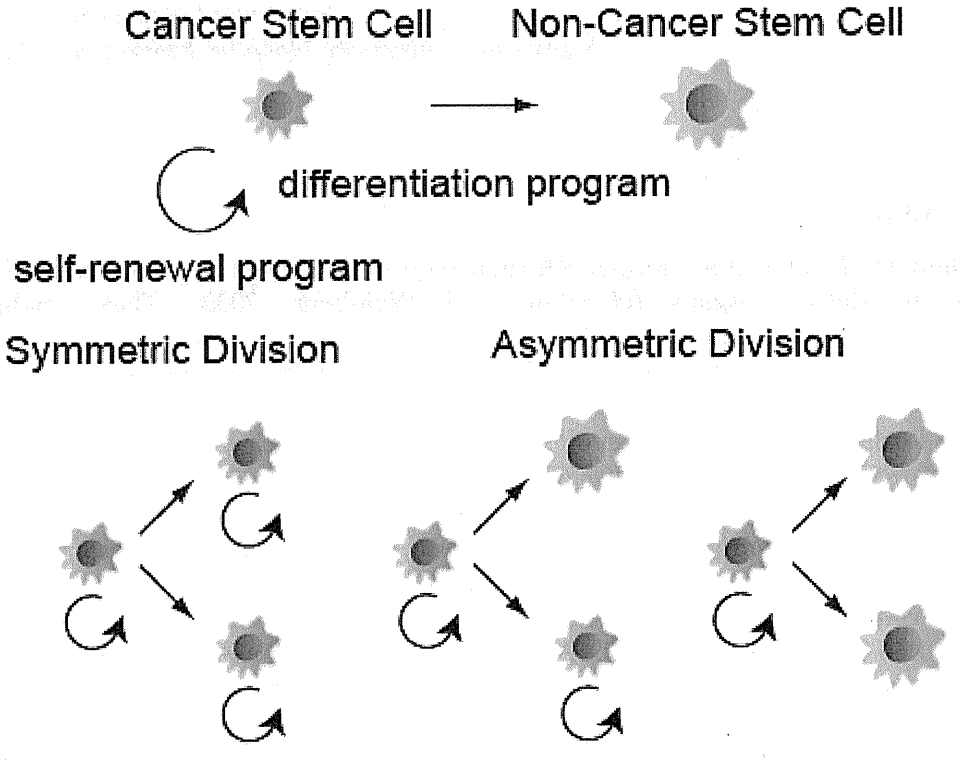

Fig. 1. Symmetric/asymmetric division of a cancer stem cell

Asymmetric cell division could be defined by the generation of one cancer stem cell and one progenitor cell with the loss of self-renewal capacity (Fig. 1 lower right panel). If both progenitors derived from a cancer stem cell lose the capacity of self-renewal by the induction of differentiation, the cancer stem cell population would be depleted and the tumor would subsequently shrink, according to the conventional cancer stem cell model.

2.1 Signaling pathways responsible for the self-renewal of cancer stem cells

A growing body of evidence suggests the similarities of normal stem cells and cancer stem cells in terms of their self-renewal and differentiation programs. Indeed, the self-renewal and differentiation programs in cancer stem cells are considered to be regulated by several signaling pathways that are activated in normal stem cells (Lobo et al., 2007). These signaling pathways seem to be activated during the process of normal organogenesis as well as carcinogenesis in a tissue-dependent manner (Pardal et al., 2003). Therefore, underscoring the significance of these signaling pathways on self-renewal and differentiation is critical for the development of treatment strategies specifically targeting cancer stem cells.

2.1.1 Wnt/β-catenin signaling

Wnt/β-catenin signaling has been studied primarily in developing embryos and was demonstrated to modulate cell proliferation, migration, and differentiation in a cellular context-dependent manner (Decaens et al., 2008; Giles et al., 2003; Moon et al., 2004; Ober et al., 2006). Wnt signaling is involved in the decision of stem cells to self-renew or differentiate during organogenesis, involving, for example, skin, intestine, bone marrow, kidney, and liver development (Moon et al., 2004; Thompson and Monga, 2007). Moreover, mutations of genes involved in Wnt/β-catenin signaling have been reported in a wide variety of human cancers including colorectal cancer, gastric cancer, skin cancer, ovarian cancer, liver cancer, and leukemia (Giles et al., 2003; Merle et al., 2005; Takebe et al., 2010; Tan et al., 2008; Vermeulen et al., 2010; Woodward et al., 2007; Zhao et al., 2007).

Wnt signaling is mediated through a core set of proteins to activate the transcriptional programs responsible for cell proliferation and development (Fig. 2). In the absence of Wnt proteins, β-catenin is phosphorylated and degraded by the Axin-APC-GSK3β complex. Once Wnt proteins bind to their receptor, Frizzled, the degradation complex is inactivated to stabilize β-catenin, which leads to its accumulation in the nucleus and interaction with T-cell factor (TCF) to activate the transcription of target genes (Moon et al., 2004).

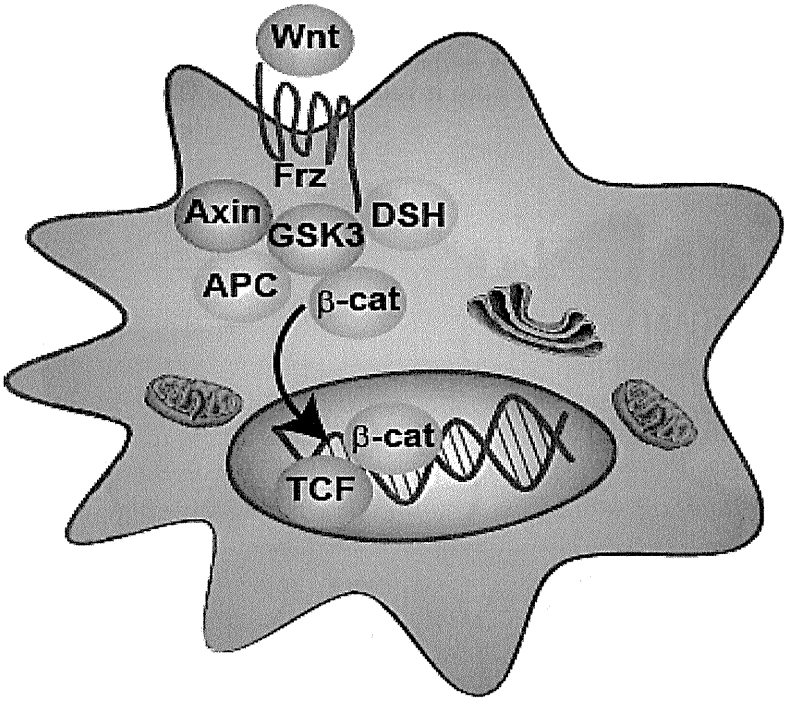

Fig. 2. Wnt/β-catenin signaling. APC, adenomatous polyposis coli; β-cat, β-catenin; DSH, Dishevelled; Frz, Frizzled; GSK3, glycogen synthase kinase 3; TCF, T-cell factor

Recent studies have demonstrated that Wnt/β-catenin signaling also plays a role in the maintenance of cancer stem cells, including colorectal cancer (Vermeulen et al., 2010), breast cancer (Li et al., 2003; Woodward et al., 2007), and liver cancer (Yang et al., 2008). We have recently demonstrated that Wnt/β-catenin signaling augments self-renewal and inhibits the differentiation of liver cancer stem cells by the expression of the stem cell marker EpCAM, which results in the enrichment of the tumor-initiating cell population (Yamashita et al.,

2008a; Yamashita et al., 2009). We have further demonstrated that small molecules, which specifically inhibit the transcriptional activity of the TCF/β-catenin complex, can suppress the cell proliferation of EpCAM-positive liver cancer cell lines, suggesting the utility of these compounds for the eradication of cancers via the inactivation of Wnt/β-catenin signaling (Yamashita et al., 2007).

2.1.2 Hedgehog signaling

The Hedgehog signaling pathway was initially identified as a regulator of segmental patterning in *Drosophila* (Nusslein-Volhard and Wieschaus, 1980). Hedgehog signaling is activated in developing embryos, especially in the skeleton and neural tube, and regulates the cell proliferation, migration, and differentiation of stem cells (Varjosalo and Taipale, 2008). Several types of cancers are reported to have an activated hedgehog signaling pathway, including glioma (Clement et al., 2007), prostate cancer (Sanchez et al., 2005), breast cancer (Liu et al., 2006), pancreatic cancer (Li et al., 2007), and hematological malignancies (Zhao et al., 2009).

Hedgehog signaling is regulated by several proteins, including ligands (Sonic Hedgehog, Desert Hedgehog, and Indian Hedgehog), the Patched (Ptch) receptor, the Smoothened (Smo) transmembrane protein, and the zinc finger transcription factor Gli (Merchant and Matsui, 2010) (Fig. 3). In the absence of ligands, Ptch represses the activity of Smo and the Gli-mediated transcriptional program is constitutively suppressed (Gli- suppressed). Once ligands bind to Ptch, the repression of Smo is released and the Gli-mediated transcriptional program is activated (Gli-activated).

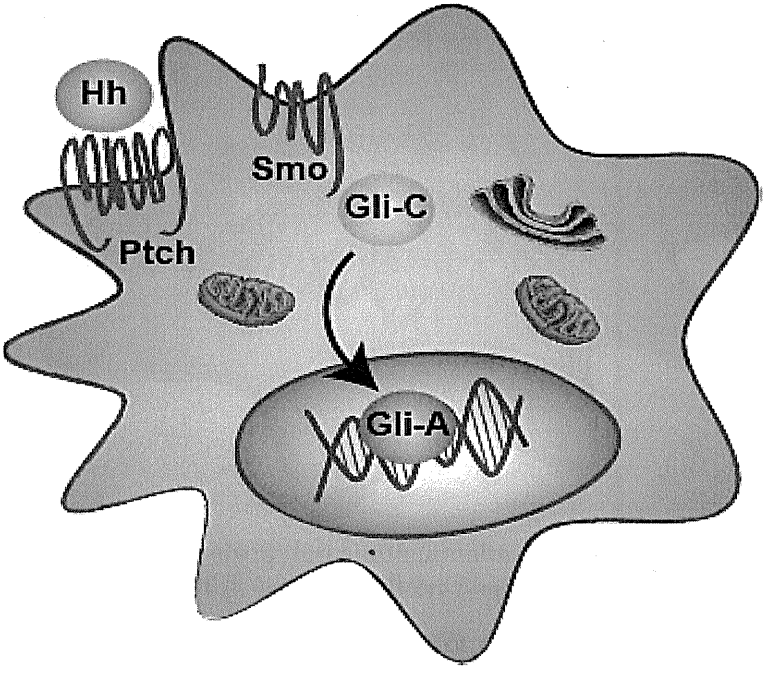

Fig. 3. Hedgehog signaling. Gli-C, Gli complex; Gli-A, Gli-activated; Hh, Hedgehog; Ptch, Patched; Smo, Smoothened

Accumulating evidence suggests that Hedgehog signaling regulates the self-renewal of cancer stem cells in several types of cancer, including glioblastoma and leukemia (Clement

et al., 2007; Zhao et al., 2009). Accordingly, Hedgehog signaling inhibitors have been clinically tested and might be beneficial for patients with advanced medulloblastoma or basal cell carcinoma, although Smo mutations in cancer cells confer resistance against such inhibitors (Rudin et al., 2009; Von Hoff et al., 2009; Yauch et al., 2009).

2.1.3 Notch signaling

Notch signaling has a pivotal role in regulating cell-to-cell communication during embryogenesis (Artavanis-Tsakonas et al., 1999), and is known to regulate stem cell fate in various organs (Androutsellis-Theotokis et al., 2006; Fre et al., 2005). Mammalian Notch ligands consist of the two structurally distinct families Delta-like ligands (DLLs) and Jagged ligands (JAGs), and these ligands are bound to the cell membrane (Fig. 4). The activation of Notch signaling is initiated by the binding of these membrane-bound ligands to Notch receptors, which results in the release of the Notch intracellular domain into the cytoplasm and nucleus by the γ-secretase complex to activate the Notch-specific transcriptional program.

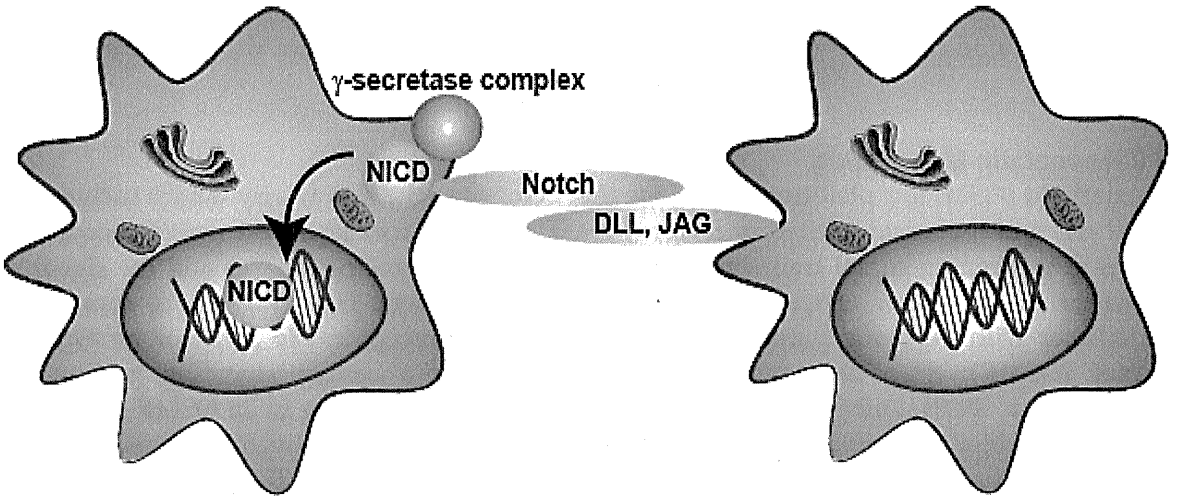

Fig. 4. Notch signaling. DLL, Delta-like ligand; JAG, Jagged; NICD, Notch intracellular domain

Notch signaling has been implicated in various types of cancers, including solid tumors and leukemia (Pannuti et al., 2010). A growing number of recent studies has demonstrated that the activation of the Notch signaling pathway can drive tumor growth via the expansion of the cancer stem cell population (Korkaya and Wicha, 2009; Peacock and Watkins, 2008; Wilson and Radtke, 2006). Indeed, the Notch signaling pathway has been demonstrated to be active in cancer stem cells and to play a critical role in the self-renewal of cancer stem cells (Fan and Eberhart, 2008; Fan et al., 2010; Wang et al., 2009). Thus, Notch signaling is considered to be a good target for pharmacological inhibition to eradicate cancer stem cells, and the effect of Notch inhibitors against Notch, including γ-secretase inhibitors or monoclonal antibodies, have been extensively evaluated (Pannuti et al., 2010).

2.2 Signaling pathways responsible for cancer stem cell differentiation

Although self-renewal pathways are considered to be critical targets for the eradication of cancer stem cells, it is still debatable if differentiation pathways are equally effective for their

eradication. Several recent studies have provided evidence of the utility and limitation of the cancer stem cell differentiation strategy by modulating the signaling pathways responsible for the differentiation of normal stem/progenitor cells.

2.2.1 Bone morphogenic protein signaling

Bone morphogenic protein (BMP) signaling is known to be activated during embryogenesis and to play a pivotal role in the differentiation of neural and intestinal stem cells (Varga and Wrana, 2005). BMPs belong to a subgroup of the transforming growth factor-β superfamily and activate signaling through the BMP-receptor (BMPR)-mediated phosphorylation of Smad proteins. Interestingly, recent studies have suggested the utility of BMPs to induce the differentiation of brain cancer stem cells and facilitate brain tumor eradication (Lee et al., 2008; Piccirillo et al., 2006). More recently, colorectal cancer stem cells have been shown to lack the expression of BMP4, and the administration of BMP4 enhanced the terminal differentiation, apoptosis, and chemosensitization of colorectal cancer stem cells (Lombardo et al., 2011). Interestingly, the effects of BMP4 on the differentiation of colorectal cancer stem cells appeared to be independent of the phosphorylation status of Smad, suggesting the importance of non-canonical signaling pathways activated by BMP4 for the differentiation of these cells.

2.2.2 Oncostatin M signaling

Oncostatin M (OSM) is a pleiotropic cytokine that belongs to the IL-6 family, which includes IL-6, IL-11, and leukemia inhibitory factor (LIF). These cytokines share the gp130 receptor subunit as a common signal transducer, and activate Janus tyrosine kinases and the signal transducer and activator of transcription 3 (STAT3) pathways. However, gp130 forms a heterodimer with a unique partner, for example, the IL6 receptor, LIF receptor, or OSM receptor (OSMR); thus, each cytokine uniquely induces a certain signaling pathway (Heinrich et al., 2003), and OSM is known to exploit distinct signaling in an OSMR-specific manner (Kinoshita and Miyajima, 2002). Of note, OSM is known to activate the hepatocytic differentiation program in hepatoblasts in an OSMR-specific manner (Kamiya et al., 1999; Kinoshita and Miyajima, 2002).

We recently identified that OSMR is expressed in a subset of liver cancer stem cells (Yamashita et al., 2010). Interestingly, OSMR-positive hepatocellular carcinoma (HCC) was characterized by the abundant expression of stem cell markers and poorly differentiated morphology, suggesting that OSMR is more likely to be expressed in HCC with stem/progenitor cell features (Yamashita et al., 2008a). Of note, the OSM-OSMR signaling pathway was maintained in these HCCs, and OSM induced hepatocytic differentiation in liver cancer stem cells (Fig. 5).

Unexpectedly, we identified that the hepatocytic differentiation of liver cancer stem cells by OSM resulted in enhanced cell proliferation *in vitro* and modest anti-tumor activity *in vivo* when administered alone. However, we have further demonstrated that OSM-mediated hepatocytic differentiation of liver cancer stem cells effectively suppresses HCC growth when combined with conventional chemotherapy. It is possible that OSM may boost the anti-tumor activity of 5-FU by "exhausting dormant cancer stem cells" through hepatocytic differentiation and active cell division (Fig. 6). A similar chemosensitization effect was observed in colorectal cancer stem cells differentiated by BMP4 administration (Lombardo et al., 2011).